UNIVERSITY OF AMSTERDAM

UvA-DARE (Digital Academic Repository)

Observation of the associated production of a top quark and a Z boson in pp collisions at √s = 13 TeV with the ATLAS detector

The ATLAS Collaboration

DOI
10.1007/JHEP07(2020)124

Publication date
2020

Document Version
Final published version

Published in
Journal of High Energy Physics

License
CC BY

Link to publication

Citation for published version (APA):
The ATLAS Collaboration (2020). Observation of the associated production of a top quark and a Z boson in *pp* collisions at $\sqrt{s}$ = 13 TeV with the ATLAS detector. *Journal of High Energy Physics*, *2020*(7), Article 124. https://doi.org/10.1007/JHEP07(2020)124

General rights
It is not permitted to download or to forward/distribute the text or part of it without the consent of the author(s) and/or copyright holder(s), other than for strictly personal, individual use, unless the work is under an open content license (like Creative Commons).

Disclaimer/Complaints regulations
If you believe that digital publication of certain material infringes any of your rights or (privacy) interests, please let the Library know, stating your reasons. In case of a legitimate complaint, the Library will make the material inaccessible and/or remove it from the website. Please Ask the Library: https://uba.uva.nl/en/contact, or a letter to: Library of the University of Amsterdam, Secretariat, P.O. Box 19185, 1000 GD Amsterdam, The Netherlands. You will be contacted as soon as possible.

UvA-DARE is a service provided by the library of the University of Amsterdam (https://dare.uva.nl)

Download date:14 Sep 2026

Published for SISSA by Springer

Received: *February 19, 2020*
Accepted: *June 10, 2020*
Published: *July 20, 2020*

Observation of the associated production of a top quark and a Z boson in pp collisions at $\sqrt{s} = 13$ TeV with the ATLAS detector

The ATLAS collaboration

E-mail: atlas.publications@cern.ch

Abstract: Single top-quark production in association with a Z boson, where the Z boson decays to a pair of charged leptons, is measured in the trilepton channel. The proton-proton collision data collected by the ATLAS experiment from 2015 to 2018 at a centre-of-mass energy of 13 TeV are used, corresponding to an integrated luminosity of 139 fb^{-1}. Events containing three isolated charged leptons (electrons or muons) and two or three jets, one of which is identified as containing a b-hadron, are selected. The main backgrounds are from $t\bar{t}Z$ and diboson production. Neural networks are used to improve the background rejection and extract the signal. The measured cross-section for $t\ell^+\ell^-q$ production, including non-resonant dilepton pairs with $m_{\ell^+\ell^-} > 30$ GeV, is 97 $\pm$ 13 (stat.) $\pm$ 7 (syst.) fb, consistent with the Standard Model prediction.

Keywords: Hadron-Hadron scattering (experiments)

ArXiv ePrint: 2002.07546

Open Access, Copyright CERN,
for the benefit of the ATLAS Collaboration.
Article funded by SCOAP^3.

https://doi.org/10.1007/JHEP07(2020)124

Contents

1 Introduction 1

2 ATLAS detector 2

3 Data and simulation samples 3

4 Object reconstruction 6

5 Signal and control regions 7

6 Background estimation 9

7 Multivariate analysis 10

8 Systematic uncertainties 12

9 Results 14

10 Conclusion 21

A Validation regions 22

The ATLAS collaboration 29

JHEP07(2020)124

1 Introduction

This paper reports on the observation of the electroweak production of a top quark or an anti-top quark associated with a Z boson (tZq) by the ATLAS collaboration using a data sample corresponding to an integrated luminosity of $139\,\text{fb}^{-1}$ of proton-proton (pp) collisions at a centre-of-mass energy of $\sqrt{s} = 13\,\text{TeV}$. The final state is where the Z boson decays into electrons or muons, and the W boson, from the top-quark decay, decays into an electron or muon and an associated neutrino, and also includes the contribution from τ-lepton decays into electrons or muons. The requirement of three leptons in the final state maximises the signal significance relative to the backgrounds. Evidence for this process has previously been reported by the ATLAS collaboration [1] with a significance of 4.2 standard deviations using data collected in 2015 and 2016. The CMS collaboration [2] reported an observation with a measured cross-section uncertainty of 15% using data collected in 2016 and 2017.

At leading order (LO) in the Standard Model (SM) both the single top-quark production and decay occur through the electroweak interaction. The main LO Feynman

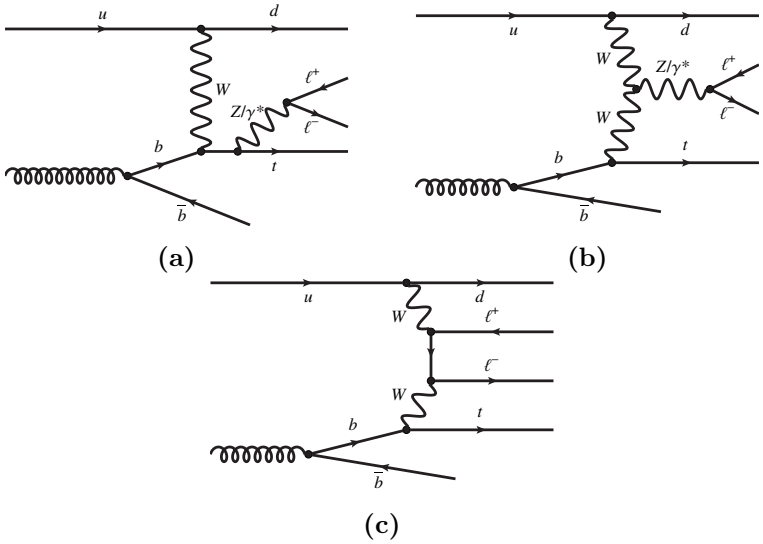

Figure 1. Example Feynman diagrams of the lowest-order amplitudes for the tZq process, corresponding to (a, b) resonant $\ell^+\ell^-$ production and (c) non-resonant $\ell^+\ell^-$ production. In the four-flavour scheme, the b-quark originates from gluon splitting.

diagram is the same as in t-channel single top-quark production with the addition of a Z boson radiated from any of the quarks (figure 1a) or from the t-channel W-boson propagator (figure 1b). This allows the t-Z and the W-Z couplings to be indirectly studied in a single interaction. At LO the $t\bar{t}Z$ process is $O(\alpha_s^2)$ in QCD, and the extraction of the t-Z coupling is more sensitive to higher-order QCD corrections. Furthermore, for the tZq process the next-to-leading-order (NLO) QCD corrections are small and therefore deviations from the SM can easily be studied in the framework of the SM effective field theory [3].

In addition to resonant Z-boson production, a small non-resonant $\ell^+\ell^-$ (with $\ell = e$, μ, τ) contribution to this process ($t\ell^+\ell^-q$) is accounted for (figure 1c). Throughout this paper, single top-quark production with either resonant or non-resonant $\ell^+\ell^-$ in the final state is referred to as tZq. In the SM, the expected cross-section for this process, calculated at NLO in QCD for a dilepton mass greater than 30 GeV, is 102^{+5}_{-2} fb.

2 ATLAS detector

The ATLAS detector [4] at the LHC covers nearly the entire solid angle around the collision point.[1] It consists of an inner tracking detector surrounded by a thin superconducting solenoid, electromagnetic and hadronic calorimeters, and a muon spectrometer incorporating three large superconducting toroidal magnets.

[1] ATLAS uses a right-handed coordinate system with its origin at the nominal interaction point (IP) in the centre of the detector and the z-axis along the beam pipe. The x-axis points from the IP to the centre of the LHC ring, and the y-axis points upwards. Cylindrical coordinates (r, ϕ) are used in the transverse plane, ϕ being the azimuthal angle around the z-axis. The pseudorapidity is defined in terms of the polar angle θ as $\eta = -\ln\tan(\theta/2)$. Distances in the η–ϕ plane are measured in units of $\Delta R \equiv \sqrt{(\Delta\eta)^2 + (\Delta\phi)^2}$.

JHEP07(2020)124

The inner-detector system (ID) is immersed in a 2 T axial magnetic field and provides charged-particle tracking in the range $|\eta| < 2.5$. The high-granularity silicon pixel detector covers the vertex region and typically provides four measurements per track, the first hit being normally in the insertable B-layer installed before Run 2 [5, 6]. It is followed by the silicon microstrip tracker, which usually provides eight measurements per track. These silicon detectors are complemented by the transition radiation tracker (TRT), which enables radially extended track reconstruction up to $|\eta| = 2.0$. The TRT also provides electron identification information based on the fraction of hits (typically 30 in total) above a higher energy-deposit threshold corresponding to transition radiation.

The calorimeter system covers the pseudorapidity range $|\eta| < 4.9$. Within the region $|\eta| < 3.2$, electromagnetic (EM) calorimetry is provided by barrel and endcap high-granularity lead/liquid-argon (LAr) calorimeters, with an additional thin LAr presampler covering $|\eta| < 1.8$, to correct for energy loss in material upstream of the calorimeters. Hadronic calorimetry is provided by the steel/scintillator-tile calorimeter, segmented into three barrel structures within the region $|\eta| < 1.7$, and two copper/LAr hadronic endcap calorimeters. The solid angle coverage is completed with forward copper/LAr and tungsten/LAr calorimeter modules optimised for electromagnetic and hadronic measurements respectively.

The muon spectrometer comprises separate trigger and high-precision tracking chambers measuring the deflection of muons in a magnetic field generated by superconducting air-core toroids. The field integral of the toroids ranges between 2.0 and 6.0 T m across most of the detector. A set of precision chambers covers the region $|\eta| < 2.7$ with three layers of monitored drift tubes, complemented by cathode-strip chambers in the forward region, where the background is highest. The muon trigger system covers the range $|\eta| < 2.4$ with resistive-plate chambers in the barrel and thin-gap chambers in the endcap regions.

Interesting events are selected for recording by the first-level trigger system implemented in custom hardware, followed by selections made by algorithms implemented in software in the high-level trigger [7]. The first-level trigger selects events from the 40 MHz bunch crossings at a rate below 100 kHz, which the high-level trigger further reduces to record events to disk at about 1 kHz.

3 Data and simulation samples

The data sample used in this article corresponds to 139 fb^{-1} of pp collisions at $\sqrt{s} = 13$ TeV collected by the ATLAS detector during 2015–2018, after requiring stable LHC beams and that all detector subsystems were operational [8].

Candidate events were required to satisfy one of the single-electron triggers or one of the single-muon triggers [7, 9–13]. Single-lepton triggers with low transverse momentum, p_{T}, thresholds and standard isolation requirements were combined in a logical OR with higher-threshold triggers that had a looser identification criterion and did not have any isolation requirement, resulting in an efficiency of almost 100% for events passing the analysis selection. The lowest p_{T} threshold used for electrons was 24 GeV (26 GeV) in 2015 (2016–2018), while for muons the threshold was 20 GeV (26 GeV).

JHEP07(2020)124

To evaluate the effects of the detector resolution and acceptance on the signal and background, and to estimate the SM backgrounds, simulated event samples were produced using a GEANT4-based Monte Carlo (MC) detector simulation [14, 15]. Some of the samples used for evaluating systematic uncertainties did not use the full GEANT4 simulation but instead relied on parameterised showers in the calorimeter. The top-quark mass in the event generators described below was set to 172.5 GeV.

The simulated data must account for the fact that significantly more than one inelastic pp collision occurs per bunch crossing. The average number of collisions per bunch crossing ranged from 13 to 38 for the 2015 through 2018 data-taking periods, respectively. Inelastic collisions were simulated using PYTHIA 8.186 [16] with the A3 set of tuned parameters [17] and the NNPDF2.3 LO [18] set of parton distribution functions (PDFs), and overlaid on the signal and background MC samples. These simulated events were reweighted to match the conditions of the collision data, specifically the additional pp interactions (pileup).

To estimate the signal acceptance and efficiency, and to study the effect of different selection criteria on the expected precision of the measurement, a tZq sample was simulated, including non-resonant $\ell^+\ell^-$ contributions. The sample was generated using the four-flavour scheme at NLO in QCD with MADGRAPH5_aMC@NLO 2.6.0 [19], requiring the dilepton invariant mass to be larger than 30 GeV and using the NNPDF30_NLO_AS_0118_NF_4 [20] PDF set. Following the discussion in ref. [21], the functional form of the renormalisation and factorisation scale was set to $4\sqrt{m_b^2 + p_{\mathrm{T},b}^2}$, where the b-quark is the one produced in the gluon splitting in the initial state associated with tZq production. The parton showering and hadronisation in signal events were simulated using PYTHIA 8.230 [22], with a set of tuned parameters selected according to ref. [23], referred to as the "A14 tune".

The predicted cross-section was calculated with MADGRAPH5_aMC@NLO 2.6.0, using the five-flavour scheme with the NNPDF30_NLO_AS_0118 PDF set and with the renormalisation and factorisation scales, μ_{R} and μ_{F}, set to $\mu_{\mathrm{R}} = \mu_{\mathrm{F}} = (m_t + m_Z)/4 = 66$ GeV. The SM tZq cross-section at NLO in QCD, including non-resonant contributions with $m_{\ell^+\ell^-} > 30$ GeV, is 102 fb. The renormalisation and factorisation scale uncertainties are $^{+5.2}_{-1.3}$% and the PDF uncertainty is ±1.0%. The PDF uncertainty was calculated using the replica method described in ref. [24].

The background to the signal is estimated by using simulated samples that contain at least two leptons and at least two jets. These samples include the production of $t\bar{t}$, $t\bar{t}H$, $t\bar{t}Z$, $t\bar{t}W$, tW, tWZ, diboson (WW, WZ, or ZZ), and Z + jets events.

The nominal $t\bar{t}$ and $t\bar{t}H$ simulated samples were generated using the NLO matrix-element generator POWHEG-BOX v2 [25–29] with the parameter h_{damp}, which controls the transverse momentum of the first additional gluon emission beyond the Born configuration, set to $1.5 \times m_t$ for $t\bar{t}$ [30] and $0.75 \times (2 \times m_t + m_H)$ for $t\bar{t}H$, with $m_H = 125$ GeV. These events were then passed through PYTHIA 8.230 to generate the underlying event and perform the parton showering and hadronisation. The PDF set used in the sample simulation was NNPDF3.0 NLO and for PYTHIA 8 the A14 tune and NNPDF2.3 LO PDF set were used.

JHEP07(2020)124

Additional $t\bar{t}$ simulated samples are used to assess modelling uncertainties [31]. To evaluate the uncertainty due to initial-state radiation, samples with higher parton radiation were produced by decreasing the factorisation and renormalisation scales by a factor of 0.5 and simultaneously increasing the h_{damp} parameter to twice its nominal value, and using the "Var3c" up variation from the A14 tune [32]. For lower parton radiation, the nominal h_{damp} value was used, while the renormalisation and factorisation scales were increased by a factor of two and the "Var3c" down variation was selected in the parton shower. To study the impact of using an alternative parton shower and hadronisation model, a sample was produced with the Powheg-Box v2 generator interfaced to Herwig 7.0.4 [33, 34], the former using the NNPDF3.0 NLO PDF set and the latter using the H7UE set of tuned parameters [34] and the MMHT2014 LO PDF set [35]. To assess the uncertainty due to the choice of matching scheme, a sample generated by MadGraph5_aMC@NLO 2.6.0 with the NNPDF3.0 NLO PDF set was passed through Pythia 8.230, which used the A14 tune and NNPDF2.3 LO PDF set. For all samples produced with this set of generators, the matrix-element correction for the first emission was turned off and the global recoil option was used.

The production of $t\bar{t}Z$ and $t\bar{t}W$ events was modelled using the MadGraph5_aMC@NLO 2.3.3 generator at NLO in QCD, with the NNPDF3.0 NLO PDF set. Parton showering and hadronisation were modelled with Pythia 8.210, using the A14 tune and the NNPDF2.3 LO PDF set. Non-resonant $\ell^+\ell^-$ contributions are included for $t\bar{t}Z$.

To assess modelling uncertainties, alternative $t\bar{t}Z$ simulated samples were produced with the Sherpa 2.2.1 [36] generator with one additional parton at NLO accuracy. The CKKW matching scale of the additional emissions was set to 30 GeV. The default Sherpa 2.2.1 parton shower was used along with the NNPDF3.0 NNLO PDF set.

The tW simulated samples used the same generators as those used for the various $t\bar{t}$ samples [37]. To avoid overlap between tW and $t\bar{t}$ production, the diagram removal (DR) scheme was employed [38], where all NLO diagrams that overlap with the doubly resonant $t\bar{t}$ contributions are removed from the calculation of the tW amplitude.

The production of tWZ events was modelled using the MadGraph5_aMC@NLO 2.3.3 generator at NLO with the NNPDF3.0 NLO PDF set. The generator was interfaced to Pythia 8.212, which used the A14 tune and the NNPDF2.3 LO PDF set. The modelling uncertainties for this process are evaluated by comparing with a MC sample produced using the same generators but employing a different treatment of the interference between $t\bar{t}Z$ and tWZ, namely the diagram removal scheme that takes the interference term into account (DR2), as opposed to the nominal DR1 scheme [39].

The simulation of the diboson event samples used the NLO Sherpa event generators: Sherpa 2.2.1 for events with one boson decaying into hadrons, and Sherpa 2.2.2 for events with both bosons decaying into leptons. In this set-up, multiple matrix elements were matched and merged with the Sherpa parton shower based on Catani-Seymour dipole factorisation [40, 41] using the MEPS@NLO prescription [42–45]. The simulations included up to one additional parton at NLO accuracy and up to three additional parton emissions at LO accuracy. The virtual QCD corrections for matrix elements at NLO accuracy were provided by the OpenLoops library [46, 47] with the NNPDF3.0 NLO PDF set.

JHEP07(2020)124

To assess modelling uncertainties for the diboson background, the POWHEG-BOX v2 [48] generator was used to generate the diboson processes at NLO in QCD. Events were generated using the CT10 NLO PDF set [49] and showered with PYTHIA 8.210 with the AZNLO [50] tune and the CTEQ6L1 [51] PDF set.

For the modelling of $Z+$jets, a sample was generated using SHERPA 2.2.1 with the NNPDF3.0 NNLO PDF set. The matching and merging procedure, as well as the virtual QCD corrections, were similar to those described for the diboson event simulation. The simulations included up to two additional partons at NLO accuracy and up to four additional parton emissions at LO accuracy.

4 Object reconstruction

The reconstruction of the basic objects used in the analysis is described in the following. The primary vertex [52] is selected as the pp vertex candidate with the highest sum of the squared transverse momenta of all associated tracks with $p_{\mathrm{T}} > 400\,\mathrm{MeV}$.

Electron candidates are reconstructed from energy clusters in the EM calorimeter that match a reconstructed track [53]. The clusters are required to be within the range $|\eta| < 2.47$, excluding the transition region between the barrel and endcap calorimeters at $1.37 < |\eta| < 1.52$. Electron candidates must also satisfy a transverse energy requirement of $E_{\mathrm{T}} > 20\,\mathrm{GeV}$ [53]. A likelihood-based discriminant is constructed from a set of variables that enhance the electron selection, while rejecting photon conversions and hadrons misidentified as electrons [53]. An η- and E_{T}-dependent selection on the likelihood discriminant is applied, such that it has an 80% efficiency when used to identify electrons from Z-boson decays. Electrons are further required to be isolated using criteria based on ID tracks and topological clusters in the calorimeter, with an efficiency of 90% (99%) for $E_{\mathrm{T}} = 25\,\mathrm{GeV}$ (60 GeV). Correction factors are applied to simulated electrons to take into account the small differences in reconstruction, identification and isolation efficiencies between data and MC simulation.

Muon candidates are reconstructed by combining a reconstructed track from the inner detector with one from the muon spectrometer [54], and are required to have $p_{\mathrm{T}} > 20\,\mathrm{GeV}$ and $|\eta| < 2.5$. To reject misidentified muon candidates, primarily originating from pion and kaon decays, several quality requirements are imposed on the muon candidate. An isolation requirement based on ID tracks and topological clusters in the calorimeter is imposed, resulting in an efficiency of 90% (99%) for $p_{\mathrm{T}} = 25\,\mathrm{GeV}$ (60 GeV). The overall efficiency obtained for muons from W-boson decays in simulated $t\bar{t}$ events is 96%. Like for electrons, correction factors are applied to simulated muons to account for the small differences between data and simulation.

Jet reconstruction in the calorimeter starts from topological clustering [55] of individual calorimeter cells calibrated to the electromagnetic energy scale. The anti-k_t algorithm [56, 57], with the radius parameter set to $R = 0.4$, is used to reconstruct the jets [58]. These jets are then calibrated to the particle level by the application of a jet energy scale derived from simulation and in situ corrections based on $\sqrt{s} = 13\,\mathrm{TeV}$ data [59]. Jets are required to have $p_{\mathrm{T}} > 35\,\mathrm{GeV}$ in the region $|\eta| < 4.5$. To suppress jets arising from pileup, a discriminant

JHEP07(2020)124

called the "jet vertex tagger" (JVT) is constructed using a two-dimensional likelihood method [60]. For jets with $p_{\mathrm{T}} < 60\,\mathrm{GeV}$ and $|\eta| < 2.5$ a JVT requirement corresponding to a 92% efficiency, while rejecting 98% of jets from pileup and noise, is imposed. To reject jets at high $|\eta|$ originating from additional pp interactions, a forward jet vertex tagger (fJVT) requirement is applied [61]. All jets with $|\eta| > 2.5$ are required to satisfy the requirements of the fJVT "medium" working point. This has an efficiency of selecting hard-scattered jets of up to 97% and a pileup-jet efficiency of 53% for jets with a p_{T} of 40 GeV.

To identify jets containing a b-hadron (b-jets), a multivariate algorithm is employed [62, 63]. It uses impact parameter and reconstructed secondary vertex information from tracks contained in the jet as input. A calibration in bins of p_{T} is derived at four efficiency points. Each jet is assigned a score, depending on how many of the efficiency points are passed. Due to its use of the ID, the reconstruction of b-jets is restricted to the region $|\eta| < 2.5$. Candidate b-jets must have a b-tagging discriminant value that exceeds a threshold such that a 70% b-jet selection efficiency is achieved in simulated $t\bar{t}$ events. With this criterion, the misidentification rate for light-jets, i.e. jets containing neither a b- nor a c-hadron, is 0.3%, while it is 11% for jets initiated by c-quarks. Correction factors are derived and applied to correct for differences in b-jet selection efficiency and the mistagging rates between data and MC simulation [62, 64, 65].

The missing transverse momentum, with magnitude $E_{\mathrm{T}}^{\mathrm{miss}}$, is calculated as the negative of the vector sum of the transverse momenta of all reconstructed objects. To account for the soft hadronic activity, a term including tracks associated with the primary vertex but not with any of the reconstructed objects is added to the $E_{\mathrm{T}}^{\mathrm{miss}}$ calculation [66].

To avoid cases where the detector response to a single physical object is reconstructed as two separate final-state objects, an overlap removal procedure is used. If electron and muon candidates share a track, the electron candidate is removed. After that, if the $\Delta R_{y,\phi}$ distance[2] between a jet and an electron candidate is less than 0.2, the jet is discarded. If multiple jets satisfy this requirement, only the closest jet is removed. For jet-electron distances between 0.2 and 0.4, the electron candidate is removed. If the distance between a jet and a muon candidate is less than 0.4, the muon candidate is removed if the jet has more than two associated tracks, otherwise the jet is removed.

5 Signal and control regions

The tZq final state used for this measurement comprises three charged leptons (electrons or muons), missing transverse momentum, one b-jet from the top-quark decay and an additional jet that does not satisfy the b-tagging requirement (untagged jet) and is expected to be emitted preferentially at high $|\eta|$. A second untagged jet is allowed in order to include events with QCD radiation. To help separate the tZq signal from the backgrounds that do not contain a Z boson and a top quark (diboson, $Z+$jets and $t\bar{t}$ events), both the Z-boson and the top-quark invariant masses are reconstructed.

[2] $\Delta R_{y,\phi}$ is the Lorentz-invariant distance in the rapidity-azimuthal-angle plane, defined as $\Delta R_{y,\phi} = \sqrt{(\Delta y)^2 + (\Delta\phi)^2}$.

JHEP07(2020)124

Common selections			
Exactly 3 leptons (e or μ) with $\lvert\eta\rvert < 2.5$ $p_{\mathrm{T}}(\ell_1) > 28\,\mathrm{GeV}$, $p_{\mathrm{T}}(\ell_2) > 20\,\mathrm{GeV}$, $p_{\mathrm{T}}(\ell_3) > 20\,\mathrm{GeV}$ $p_{\mathrm{T}}(\mathrm{jet}) > 35\,\mathrm{GeV}$			
SR 2j1b	CR diboson 2j0b	CR $t\bar{t}$ 2j1b	CR $t\bar{t}Z$ 3j2b
≥ 1 OSSF pair	≥ 1 OSSF pair	≥ 1 OSDF pair	≥ 1 OSSF pair
$\lvert m_{\ell\ell} - m_Z\rvert < 10\,\mathrm{GeV}$	$\lvert m_{\ell\ell} - m_Z\rvert < 10\,\mathrm{GeV}$	No OSSF pair	$\lvert m_{\ell\ell} - m_Z\rvert < 10\,\mathrm{GeV}$
2 jets, $\lvert\eta\rvert < 4.5$	2 jets, $\lvert\eta\rvert < 4.5$	2 jets, $\lvert\eta\rvert < 4.5$	3 jets, $\lvert\eta\rvert < 4.5$
1 b-jet, $\lvert\eta\rvert < 2.5$	0 b-jets	1 b-jet, $\lvert\eta\rvert < 2.5$	2 b-jets, $\lvert\eta\rvert < 2.5$
SR 3j1b	CR diboson 3j0b	CR $t\bar{t}$ 3j1b	CR $t\bar{t}Z$ 4j2b
≥ 1 OSSF pair	≥ 1 OSSF pair	≥ 1 OSDF pair	≥ 1 OSSF pair
$\lvert m_{\ell\ell} - m_Z\rvert < 10\,\mathrm{GeV}$	$\lvert m_{\ell\ell} - m_Z\rvert < 10\,\mathrm{GeV}$	No OSSF pair	$\lvert m_{\ell\ell} - m_Z\rvert < 10\,\mathrm{GeV}$
3 jets, $\lvert\eta\rvert < 4.5$	3 jets, $\lvert\eta\rvert < 4.5$	3 jets, $\lvert\eta\rvert < 4.5$	4 jets, $\lvert\eta\rvert < 4.5$
1 b-jet, $\lvert\eta\rvert < 2.5$	0 b-jets	1 b-jet, $\lvert\eta\rvert < 2.5$	2 b-jets, $\lvert\eta\rvert < 2.5$

Table 1. Overview of the requirements applied when selecting events in the signal and control regions. OSSF is an opposite-sign same-flavour lepton pair. OSDF is an opposite-sign different-flavour lepton pair.

The data are divided into eight non-overlapping regions: two signal regions (SR) designed to select tZq events and six control regions (CR) designed to enhance the selection of the main sources of background events ($t\bar{t}Z$, diboson, $Z+$jets and $t\bar{t}$ events). The CRs are used to adjust the normalisation and reduce the associated systematic uncertainties in the main backgrounds.

Table 1 summarises the selection criteria applied across all the regions considered. Leptons and jets have to satisfy the requirements discussed in section 4 and one of the leptons is required to have $p_{\mathrm{T}} > 28\,\mathrm{GeV}$, because of the trigger thresholds, and match, with $\Delta R < 0.15$, the lepton reconstructed by the trigger. The nomenclature njmb is used to denote the regions, where n is the total number of jets, of which m are b-tagged.

The SRs require an opposite-sign, same-flavour (OSSF) lepton pair to reconstruct the Z boson. In the μee and $e\mu\mu$ channels the pair is uniquely identified, whereas in the eee and $\mu\mu\mu$ channels both of the possible combinations are considered and the pair with the invariant mass closer to the Z-boson mass is chosen. The dilepton invariant mass requirement is $\lvert m_{\ell\ell} - m_Z\rvert < 10\,\mathrm{GeV}$. The remaining lepton and the $E_{\mathrm{T}}^{\mathrm{miss}}$ are used to reconstruct the leptonically decaying W boson.[3] The four-momenta of the reconstructed W boson and the b-jet are summed to reconstruct the top quark.

The diboson CRs use the same event selection as each of the SRs but a b-tag veto is applied. The CRs for $t\bar{t}Z$ are the same as the SRs except for the addition of another b-jet. The CRs for $t\bar{t}$ are the same as the SRs except for the requirement of no OSSF lepton pair and at least one opposite-sign, different-flavour (OSDF) lepton pair.

[3]The longitudinal component of the neutrino four-momentum is obtained by using the mass constraint of the W boson. The twofold ambiguity is resolved by choosing the solution with the smaller $\lvert p_z^{\nu}\rvert$, since the W boson is expected to be produced with small pseudorapidity [67].

JHEP07(2020)124

These SRs and CRs are included in a binned maximum-likelihood fit that is performed to measure the signal cross-section. In the fit, the normalisations of the signal and the $t\bar{t}$ (including tW) and $Z+$jets backgrounds are unconstrained, while the other backgrounds are constrained to be close to their SM prediction (see section 8).

6 Background estimation

Two classes of backgrounds are considered: processes in which three or more prompt leptons are produced, such as diboson production or the associated production of a top-quark pair and a boson (W, Z or H); and processes with only two prompt leptons in the final state (such as $Z+$jets, $t\bar{t}$ and tW production) and one additional non-prompt or fake lepton that satisfies the selection criteria. Such non-prompt or fake leptons can originate from decays of bottom or charm hadrons, from jets misidentified as electrons, leptons from kaon or pion decays, or electrons from photon conversions.

After applying the SR event selection, diboson, $t\bar{t}Z$, $Z+$jets and $t\bar{t}$ production constitute the largest backgrounds. For the SR 2j1b, the dominant background source is diboson production, mainly WZ events. Monte Carlo simulation indicates that these represent 50% of the total number of selected background events in this region, while the second largest backgrounds, $t\bar{t}Z$ and tWZ amount to 32%. Non-prompt-lepton backgrounds are predicted to contribute up to 14% of the events. In the SR 3j1b, $t\bar{t}Z$ is the dominant background source, giving 45% of background events. Diboson production yields 28% of all background events in that region.

The diboson contribution is split according to the origin of the associated jets using generator-level information. If one of the jets contains a b- or c-hadron then it is classified as diboson + heavy flavour ($VV+$HF), otherwise the event is classified as diboson + light flavour ($VV+$LF).

The $t\bar{t}Z$ and tWZ backgrounds are combined, as are $t\bar{t}$ and tW. The $t\bar{t}W$ and $t\bar{t}H$ contributions are also combined, since both are very small.

All background contributions involving prompt leptons are estimated by using MC samples that are normalised to their respective SM predicted cross-sections calculated at NLO in QCD. The cross-section of the $t\bar{t}H$ background includes NLO+NLL soft-gluon resummation [68].

The estimation of the non-prompt-lepton background using MC samples is challenging. The simulation does not accurately model the rate for prompt-lepton misidentification. In addition, it suffers from low statistics after applying the SR event selection requirements, leading to large fluctuations in the predicted event kinematics. The first issue is addressed by normalising the non-prompt-lepton predictions to data in dedicated CRs. The method developed to address the second issue is discussed in the following. Generator-level studies have shown that for $t\bar{t}$ events[4] and $Z+$jets events passing the event selection, the additional non-prompt lepton usually originates from a charm- or bottom-hadron decay,

[4]This is also valid for the very small number of tW events. The same method of estimating their contribution is used for both processes.

JHEP07(2020)124

with a smaller contribution from other sources, such as photon conversions in the case of non-prompt electrons.

Therefore, the method used to estimate the shape of kinematic distributions for non-prompt-lepton backgrounds with high statistical precision uses MC samples enriched in events with semileptonic b-jet decays. Generated events are used for $t\bar{t}+tW$ and $Z+$jets independently, with a preselection of two leptons instead of three leptons and two b-jets. One of the two b-jets, which is selected at random, is replaced by a lepton. The energy and polar angle of the replacement lepton, relative to the direction of the b-jet momentum, are derived from a generator-level study of the polar-angle distribution versus lepton energy in the rest frame of the b-hadron, which is assumed to carry the b-jet energy. The azimuthal angle is generated uniformly around the b-jet direction. The lepton four-momenta are transformed to the laboratory frame using the b-jet four-momenta. If the b-jet is within a cone of $\Delta R = 0.4$ around the lepton, the b-jet is removed. In the other events the b-jet is kept and the event will ultimately not satisfy the common selection, as it contains two b-jets. The distributions of kinematic variables from the resulting sample are compared with those from the $t\bar{t}+tW$ and $Z+$jets MC samples, applying the common selection, and are found to agree within statistical uncertainties.

7 Multivariate analysis

To improve the separation between signal and background, a neural network (NN) is used to derive a discriminant that takes correlations among the input variables into account. The package NeuroBayes [69, 70] is used, which combines a three-layer feed-forward NN with a complex, robust preprocessing that orders the input variables by their separation power [71]. The first layer of the network consists of one input node for each input variable plus one bias node [69]. The second layer can have an arbitrary, user-defined, number of hidden nodes. There is one output node that gives a continuous value in the interval $[-1, 1]$. The NN uses Bayesian regularisation [69] during the training process to improve its performance and stability, and to avoid overtraining. All background processes are considered in the training and are weighted according to the expected number of events in each SR.

Only variables that provide good separation and are well modelled are used in the final NN. A separate network is trained for each of the SRs, with each NN starting with the same input variables and 25 hidden nodes. The 15 input variables that give the best separation according to NeuroBayes are used for the final NN training. The full list of the variables used for the NN training is shown in table 2. The untagged jet is denoted $\mathrm{j_f}$. When two untagged jets are selected, $\mathrm{j_f}$ ($\mathrm{j_r}$) refers to the one for which the invariant mass of this untagged jet and the b-tagged jet is the largest (smallest).

Variables related to the reconstructed Z boson help to reduce the $t\bar{t}$ background, while top-quark-related quantities are useful in separating the signal from processes such as WZ and $Z+$jets, in which no top quark is produced. For the signal, the untagged jet comes from the spectator quark in the hard-scattering process and thus tends to have higher $|\eta|$, helping the NN provide better separation from diboson and $t\bar{t}Z$ background events. The

JHEP07(2020)124

Variable	Rank		Definition
	SR 2j1b	SR 3j1b	
$m_{b\mathrm{j_f}}$	1	1	(Largest) invariant mass of the b-jet and the untagged jet(s)
m_{top}	2	2	Reconstructed top-quark mass
$\lvert\eta(\mathrm{j_f})\rvert$	3	3	Absolute value of the η of the $\mathrm{j_f}$ jet
$m_{\mathrm{T}}(\ell, E_{\mathrm{T}}^{\mathrm{miss}})$	4	4	Transverse mass of the W boson
b-tagging score	5	11	b-tagging score of the b-jet
H_{T}	6	–	Scalar sum of the p_{T} of the leptons and jets in the event
$q(\ell_W)$	7	8	Electric charge of the lepton from the W-boson decay
$\lvert\eta(\ell_W)\rvert$	8	12	Absolute value of the η of the lepton from the W-boson decay
$p_{\mathrm{T}}(W)$	9	15	p_{T} of the reconstructed W boson
$p_{\mathrm{T}}(\ell_W)$	10	14	p_{T} of the lepton from the W-boson decay
$m(\ell\ell)$	11	–	Mass of the reconstructed Z boson
$\lvert\eta(Z)\rvert$	12	13	Absolute value of the η of the reconstructed Z boson
$\Delta R(\mathrm{j_f}, Z)$	13	7	ΔR between the $\mathrm{j_f}$ jet and the reconstructed Z boson
$E_{\mathrm{T}}^{\mathrm{miss}}$	14	–	Missing transverse momentum
$p_{\mathrm{T}}(\mathrm{j_f})$	15	10	p_{T} of the $\mathrm{j_f}$ jet
$\lvert\eta(\mathrm{j_r})\rvert$	–	5	Absolute value of the η of the $\mathrm{j_r}$ jet
$p_{\mathrm{T}}(Z)$	–	6	p_{T} of the reconstructed Z boson
$p_{\mathrm{T}}(\mathrm{j_r})$	–	9	p_{T} of the $\mathrm{j_r}$ jet

Table 2. Variables used as input to the neural network in SR 2j1b and SR 3j1b. The ranking of the variables in each of the SRs is given in the 2$^{\mathrm{nd}}$ and 3$^{\mathrm{rd}}$ columns, respectively. The untagged jet is denoted $\mathrm{j_f}$. When two untagged jets are selected, $\mathrm{j_f}$ ($\mathrm{j_r}$) refers to the one for which the invariant mass of this untagged jet and the b-tagged jet is the largest (smallest). The b-tagging score indicates whether the b-jet would also satisfy a tighter b-tagging requirement corresponding to a working point with an efficiency of 60% instead of 70%.

invariant mass of an untagged jet and b-jet, $m_{b\mathrm{j_f}}$, is also used as a discriminating variable for selecting signal over background.

In terms of the separation power, the four highest-ranked variables for the two SRs are the same. The highest-ranked variable is $m_{b\mathrm{j_f}}$. The $m_{b\mathrm{j_f}}$ value is larger for topologies with a forward jet, because of the large angular separation between the forward jet and the central b-jet. The other three variables are the reconstructed top-quark mass, the absolute value of the untagged $\mathrm{j_f}$ jet pseudorapidity, and the transverse mass of the W boson.[5]

The post-fit distributions of the three variables with the highest discrimination power are shown in figure 2 for the two SRs. Good agreement between data and prediction is observed.

[5]The transverse mass is calculated using the momentum of the lepton associated with the W boson, $E_{\mathrm{T}}^{\mathrm{miss}}$ and the azimuthal angle, ϕ, between the two: $m_{\mathrm{T}}\left(\ell, E_{\mathrm{T}}^{\mathrm{miss}}\right) = \sqrt{2p_{\mathrm{T}}(\ell)E_{\mathrm{T}}^{\mathrm{miss}}\left[1-\cos\Delta\phi\left(\ell, E_{\mathrm{T}}^{\mathrm{miss}}\right)\right]}$.

JHEP07(2020)124

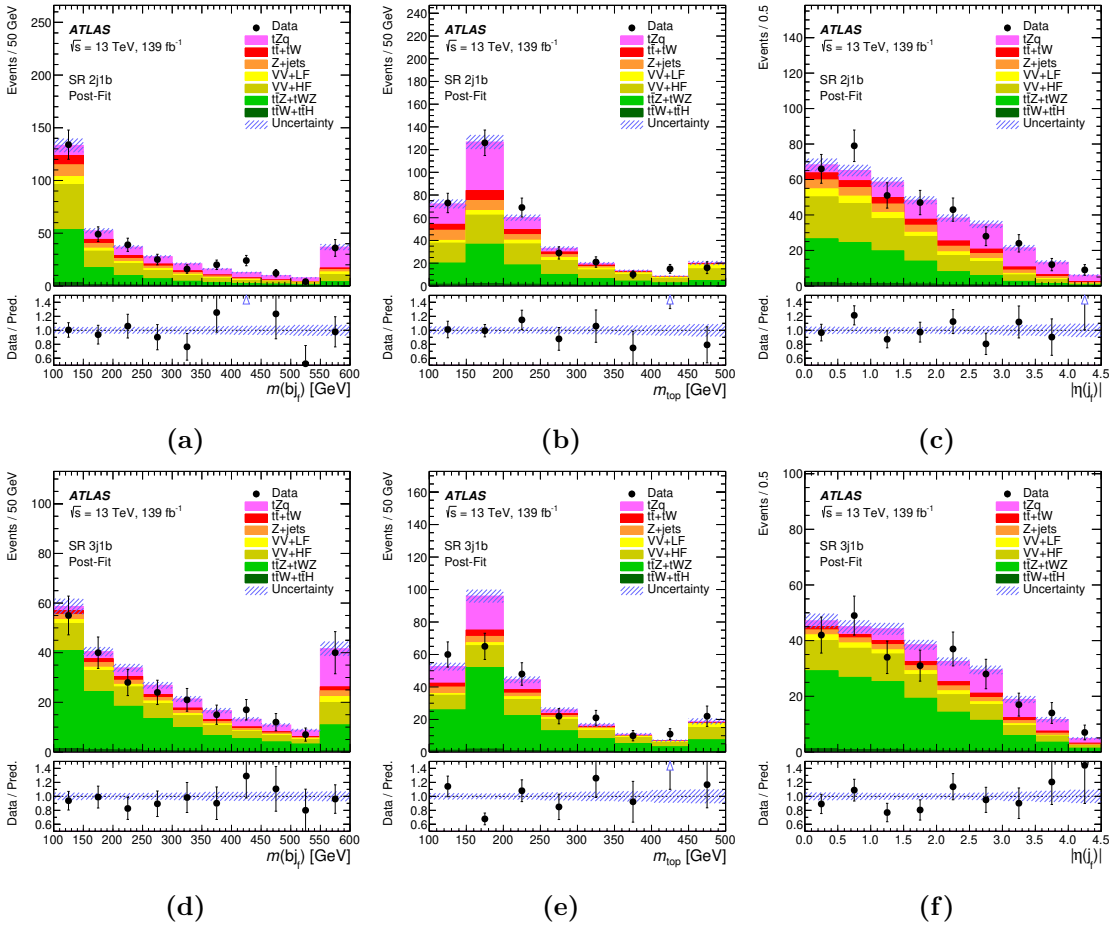

Figure 2. Comparison between data and prediction ("Pred.") for the three most discriminating NN input variables after the fit to data ("Post-Fit") under the signal-plus-background hypothesis. The variables displayed are: (a) and (d) the invariant mass of the b-jet and the untagged jet, (b) and (e) the mass of the reconstructed top quark, and (c) and (f) the absolute value of the η of the j_f jet, shown in the SR 2j1b (top row) and SR 3j1b (bottom row). The jet denoted j_f is the untagged jet for which the invariant mass of this untagged jet and the b-tagged jet is the largest. The uncertainty band includes both the statistical and systematic uncertainties as obtained by the fit. The rightmost bin includes overflow events. The lower panels show the ratios of the data to the prediction. The open triangles indicate points that are outside the vertical range of the figure.

8 Systematic uncertainties

Systematic uncertainties in the signal acceptance and in the normalisation of the individual backgrounds, as well as uncertainties in the shape of the fitted distributions, are taken into account. These are treated as correlated between the different regions, unless stated otherwise. The uncertainties can be classified into the following categories:

Reconstruction efficiency and calibration uncertainties. Systematic uncertainties affecting the reconstruction efficiency and energy calibration of electrons, muons and jets are propagated through the analysis, each contributing at the percent level to the signal and background uncertainties before the fit.

JHEP07(2020)124

The differences between the electron (muon) trigger, reconstruction and selection efficiencies in data and those in MC simulation are corrected for by scale factors derived from dedicated $Z \to e^+e^-$ ($Z \to \mu^+\mu^-$) enriched control samples using a tag-and-probe method [53, 54].

The jet energy scale (JES) was derived using information from test-beam data, LHC collision data and simulation, as described in ref. [59]. The fractional JES uncertainty decreases with the p_{T} of the reconstructed jet and is rather stable in η. It has various components according to the factors it accounts for and the different steps used to compute it. The impact of the uncertainty in the jet energy resolution is also evaluated.

The b-tagging efficiencies and mistagging rate are measured in data using the same methods as described in refs. [62, 64, 65], with the systematic uncertainties due to b-tagging efficiency and the mistagging rates calculated separately. The impact of the uncertainties on the b-tagging calibration is evaluated separately for b-, c- and light-jets in the MC samples.

The uncertainty in $E_{\mathrm{T}}^{\mathrm{miss}}$ due to a possible miscalibration of the soft-track component of the $E_{\mathrm{T}}^{\mathrm{miss}}$ is derived from data-MC comparisons of the p_{T} balance between the hard and soft $E_{\mathrm{T}}^{\mathrm{miss}}$ components [66]. The uncertainty associated with the leptons and jets is propagated from the corresponding uncertainties in the energy/momentum scales and resolutions, and is classified together with the uncertainty associated with the corresponding objects.

Signal and background modelling. The systematic uncertainties due to MC modelling of the signal and the $t\bar{t}$ and $t\bar{t}Z$ backgrounds are estimated by comparing different MC generators and by varying the parameters associated with the renormalisation and factorisation scales, and additional radiation.

For the signal MC simulation, the effects of the systematic uncertainty in the renormalisation and factorisation scales, which are set equal to each other, and in the amount of additional radiation are calculated simultaneously and are referred to as "tZq QCD radiation". This is done by increasing the scales by a factor of two and using the "Var3cDown" parameter of the A14 tune, and by decreasing the scales by a factor of 0.5 combined with the A14 tune using "Var3cUp" [23]. The PDF uncertainty in the signal MC prediction is also taken into account by calculating the RMS of the 100 replicas of the NNPDF30_nlo_as_0118_nf_4 PDF set following the PDF4LHC prescription [24]. The PDF uncertainty shape variations are very small and are therefore neglected.

The effect of changing the MC generator for $t\bar{t}$ events is included as the $t\bar{t}$ NLO matching systematic uncertainty by taking the difference between the Powheg-Box and MadGraph5_aMC@NLO predictions. The impact of changing the parton shower and hadronisation model is evaluated by comparing samples generated with Powheg-Box interfaced with either Pythia 8 or Herwig 7, as described in ref. [72]. Systematic uncertainties related to the scale and additional radiation are also included using the samples described in section 3.

The effect of changing the MC generator for $t\bar{t}Z$ events is included as the $t\bar{t}Z$ modelling systematic uncertainty by taking the difference between the MadGraph5_aMC@NLO and Sherpa predictions. Uncertainties related to the choice of renormalisation and factorisation scales, as well as initial-state radiation are also included.

JHEP07(2020)124

The uncertainty associated with the modelling of diboson events is assessed by comparing the predictions of the Sherpa and Powheg-Box generators. This uncertainty is treated as uncorrelated for the VV + LF and VV + HF components.

To account for the possible differences in the distribution shape of Z + jets events originating from sources other than semileptonic b-decays, a systematic uncertainty in the shape of the Z + jets distribution is applied. The systematic uncertainty is constructed by comparing the distribution shapes of MC events from different sources separated according to the origin of the fake lepton in the event (e.g. heavy-flavour decay, photon conversion, etc.). This uncertainty is not included for $t\bar{t}$ + tW since the non-prompt-lepton contributions in CRs and SRs have the same composition and are fully dominated by semileptonic b-decays.

Background rate uncertainty. For $t\bar{t}Z$ and tWZ productions, a cross-section uncertainty of 12% is used [73], correlated among the two processes. For VV + LF production, the normalisation uncertainty is taken to be 20% [74]. The uncertainty for VV + HF production is 30% [75]. The diboson production uncertainties are taken to be uncorrelated. In addition, modelling uncertainties are also used in the fit, as mentioned above. For $t\bar{t}W$ and $t\bar{t}H$ a 15% systematic uncertainty in the normalisation is used [73], correlated among the two processes.

For the backgrounds that are unconstrained in the fit (Z + jets and $t\bar{t}$ + tW), an additional normalisation uncertainty of 15% for Z + jets and 7% for $t\bar{t}$ + tW, uncorrelated for each region, is included to allow for differences between the regions. These values correspond to the largest statistical uncertainty in the predicted yields for the Z + jets and $t\bar{t}$ + tW MC samples in the SRs and the relevant CRs.

Luminosity. The uncertainty in the combined 2015–2018 integrated luminosity is 1.7% [76], obtained using the LUCID-2 detector [77] for the primary luminosity measurements.

Uncertainty in pileup modelling. The uncertainty in pileup modelling is accounted for by varying the reweighting of the MC samples to the data pileup conditions using the uncertainty on the average number of interactions per bunch crossing.

9 Results

A simultaneous binned maximum-likelihood fit of the SRs and CRs is performed using MC distributions for both the signal and background predictions. The templates are binned distributions of the NN output (O_{NN}) for the SRs and $t\bar{t}Z$ CRs; $m_{\text{T}}(\ell, E_{\text{T}}^{\text{miss}})$ for the diboson CR, to provide separation between diboson and Z + jets events in this region; and the total event yield in the $t\bar{t}$ CRs. For the $t\bar{t}Z$ CR templates, the NN trained in a given SR is evaluated on the events selected in the corresponding CR. In this case, the top-quark reconstruction is performed using the reconstructed W boson and b-jet combination that has the invariant mass closest to m_t. To measure the tZq cross-section the normalisation of the signal template is extracted from the fit.

JHEP07(2020)124

Nuisance parameters are included in the fit to account for each systematic variation described in section 8. When variations of the shape of the distributions are not statistically significant, only the effect on the normalisation is taken into account in the assessment of the systematic uncertainty. To quantify the statistical significance of the fit and its resulting power to reject the background-only hypothesis, a test statistic is constructed using a profile likelihood ratio.

Figures 3 and 4 show the comparison between data and post-fit background and signal distributions, in the SRs and CRs, respectively. The numbers of fitted signal and background events compared with the data are shown in table 3. The normalisation of the unconstrained fit parameters agrees with the SM predictions. Validation regions are defined to further check the level of agreement between data and simulation. Details are given in appendix A.

The results of the fit yield a tZq production cross-section, including non-resonant dilepton pairs with $m_{\ell^+\ell^-} > 30\,\text{GeV}$, of $97 \pm 13\,\text{(stat.)} \pm 7\,\text{(syst.)}\,\text{fb}$, assuming $m_t = 172.5\,\text{GeV}$, corresponding to a total uncertainty of $\pm 14\%$. The SM cross-section for this process is $102^{+5}_{-2}\,\text{fb}$. The statistical uncertainty of 13% in the measurement, which is dominant for this result, is obtained by performing the fit after fixing all nuisance parameters to their post-fit values. The systematic uncertainty is computed by subtracting in quadrature the statistical component of the uncertainty from the total. The impact of the systematic uncertainties on the tZq cross-section, broken down into major categories, is summarised in table 4.

The statistical significance of obtaining a signal at least as large as that observed in the data if no signal were present is calculated using the test statistic in the asymptotic approximation [78]. Both the expected and observed significances are well above five standard deviations.

The distributions of the reconstructed p_{T} of the top quark and of the Z boson in the SR 2j1b for events with high O_{NN} score ($O_{\text{NN}} > 0.4$) are shown in figure 5. Good agreement is observed between data and the prediction.

JHEP07(2020)124

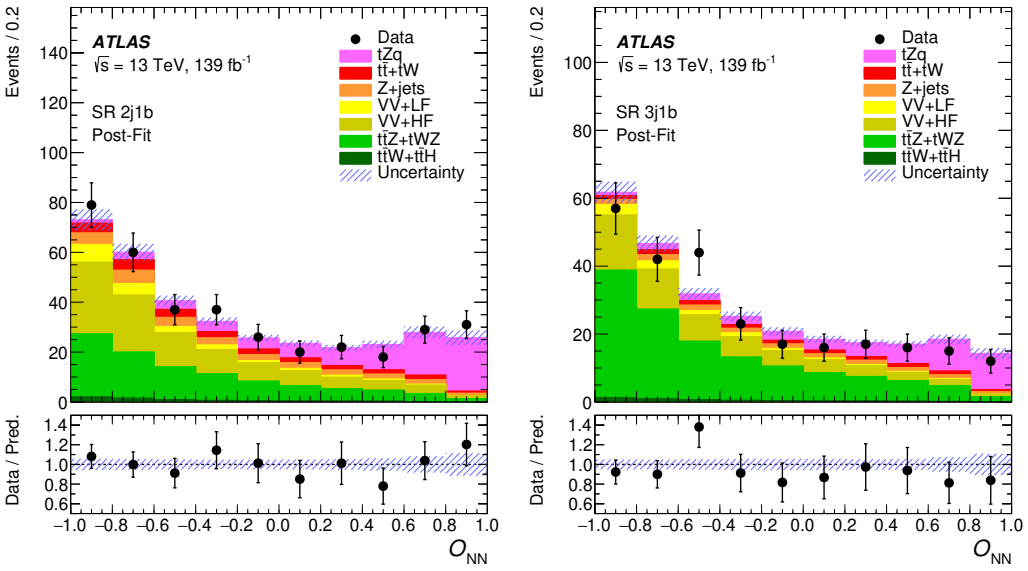

(a) **(b)**

Figure 3. Comparison between data and prediction ("Pred.") after the fit to data ("Post-Fit") under the signal-plus-background hypothesis for the fitted distributions of the neural network output O_{NN} in the SRs (a) 2j1b and (b) 3j1b. The uncertainty band includes both the statistical and systematic uncertainties as obtained by the fit. The lower panels show the ratios of the data to the prediction.

JHEP07(2020)124

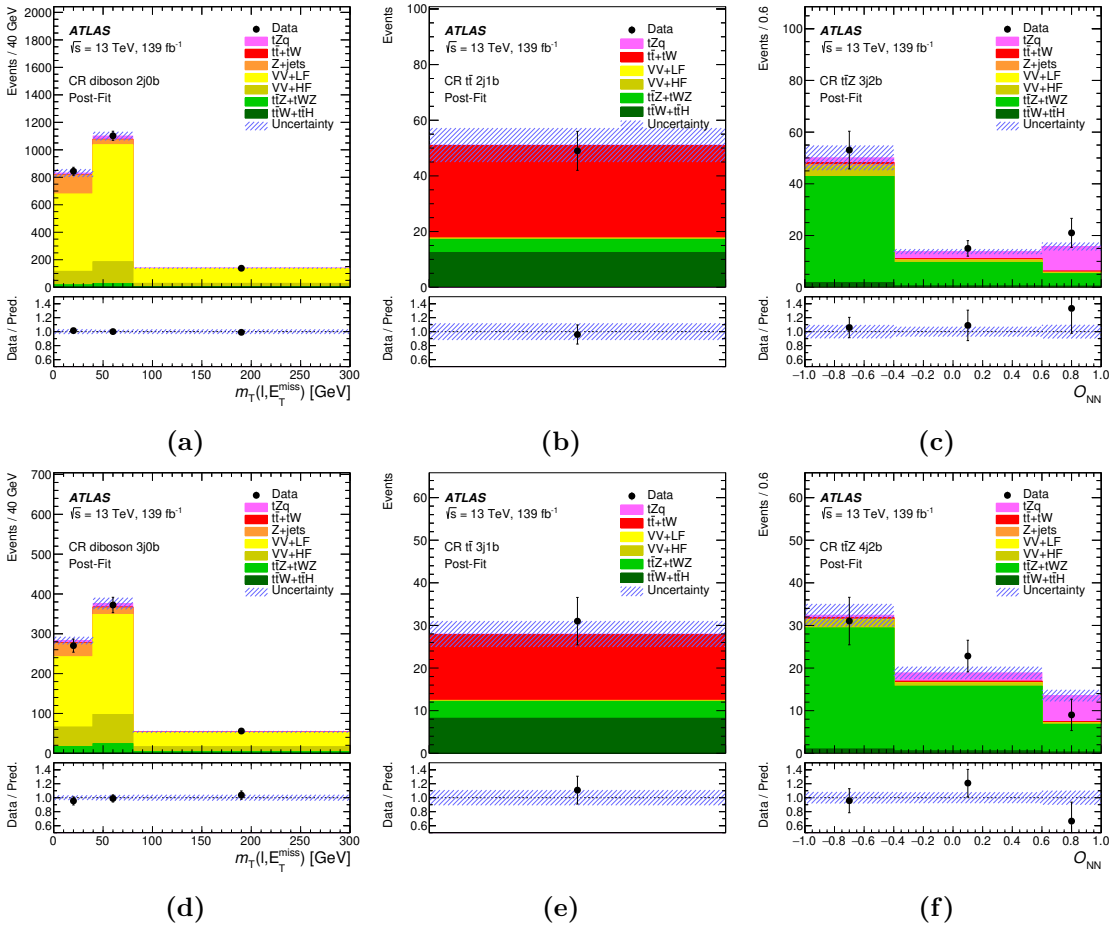

Figure 4. Comparison between data and prediction ("Pred.") after the fit to data ("Post-Fit") under the signal-plus-background hypothesis for the fitted distributions in the CRs. The fitted distributions are: (a) and (d) the $m_{\mathrm{T}}(\ell, E_{\mathrm{T}}^{\mathrm{miss}})$ distribution in the diboson CRs, (b) and (e) the event yields in the $t\bar{t}$ CRs, and (c) and (f) the O_{NN} distribution in the $t\bar{t}Z$ CRs. The uncertainty band includes both the statistical and systematic uncertainties as obtained by the fit. The lower panels show the ratios of the data to the prediction.

JHEP07(2020)124

	SR 2j1b	CR diboson 2j0b	CR $t\bar{t}$ 2j1b	CR $t\bar{t}Z$ 3j2b
tZq	79 ± 11	53.1 ± 7.5	0.2 ± 0.1	12.9 ± 2.0
$t\bar{t}$ + tW	23.8 ± 4.8	13.7 ± 2.7	33.3 ± 6.3	1.7 ± 0.3
Z + jets	28 ± 13	181 ± 82	< 0.1	1.4 ± 0.6
VV + LF	19.7 ± 7.9	2000 ± 100	< 0.1	0.1 ± 0.1
VV + HF	101 ± 22	383 ± 78	0.4 ± 0.1	5.2 ± 1.7
$t\bar{t}Z$ + tWZ	96 ± 11	63.2 ± 7.0	4.8 ± 0.5	59.3 ± 7.1
$t\bar{t}H$ + $t\bar{t}W$	6.5 ± 1.0	3.0 ± 0.5	12.4 ± 1.9	2.8 ± 0.5
Total	354 ± 16	2697 ± 56	51.1 ± 6.1	83.5 ± 6.4
Data	359	2703	49	92

	SR 3j1b	CR diboson 3j0b	CR $t\bar{t}$ 3j1b	CR $t\bar{t}Z$ 4j2b
tZq	43.4 ± 6.2	21.2 ± 3.3	0.2 ± 0.1	8.0 ± 1.3
$t\bar{t}$ + tW	11.0 ± 2.2	6.9 ± 1.3	15.4 ± 3.1	1.0 ± 0.2
Z + jets	12.8 ± 6.0	53 ± 23	< 0.1	0.4 ± 0.2
VV + LF	10.1 ± 4.2	624 ± 53	< 0.1	0.1 ± 0.1
VV + HF	58 ± 17	186 ± 51	0.3 ± 0.1	3.4 ± 1.0
$t\bar{t}Z$ + tWZ	132 ± 12	61.9 ± 6.2	3.9 ± 0.5	58.1 ± 5.3
$t\bar{t}H$ + $t\bar{t}W$	4.7 ± 0.7	1.7 ± 0.3	8.2 ± 1.3	2.0 ± 0.3
Total	272 ± 12	955 ± 29	28.0 ± 3.0	72.8 ± 5.0
Data	259	949	31	75

Table 3. Predicted and observed yields in each of the analysis regions considered. The signal and background predictions are shown after the fit to data. The quoted uncertainties include the statistical and systematic uncertainties of the yields, computed taking into account correlations among nuisance parameters and among processes.

JHEP07(2020)124

Uncertainty source	$\Delta\sigma/\sigma$ [%]
Prompt-lepton background modelling and normalisation	3.3
Jets and $E_{\mathrm{T}}^{\mathrm{miss}}$ reconstruction and calibration	2.0
Lepton reconstruction and calibration	2.0
Luminosity	1.7
Non-prompt-lepton background modelling	1.6
Pileup modelling	1.2
MC statistics	1.0
tZq modelling (QCD radiation)	0.8
tZq modelling (PDF)	0.7
Jet flavour tagging	0.4
Total systematic uncertainty	7.0
Data statistics	12.6
$t\bar{t} + tW$ and $Z +$ jets normalisation	2.1
Total statistical uncertainty	12.9

Table 4. Impact of systematic uncertainties on the tZq cross-section, broken down into major categories. For each category the impact is calculated by performing a fit where the nuisance parameters in the group are fixed to their best-fit values, and then subtracting the resulting uncertainty in the parameter of interest in quadrature from the uncertainty from the nominal fit. For simplicity, the impact is given as the average of the up and down variations. Details of the systematic uncertainties are provided in the text. MC statistics refers to the effect of the limited size of the MC samples. The total systematic uncertainty is a bit larger than the quadratic sum of the individual contributions due to correlations.

JHEP07(2020)124

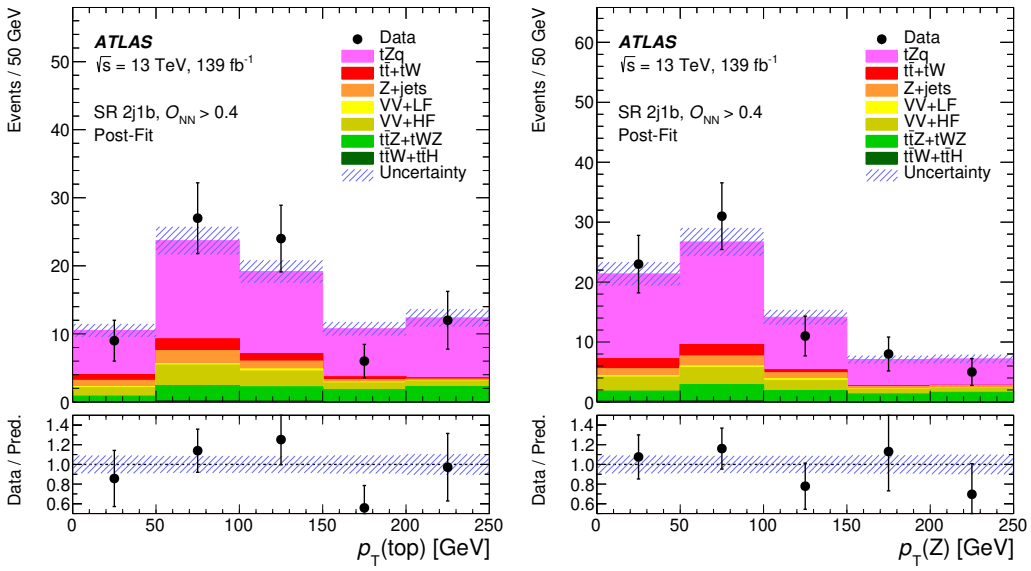

(a) **(b)**

Figure 5. Comparison between data and prediction ("Pred.") after the fit to data ("Post-Fit") under the signal-plus-background hypothesis for the reconstructed p_{T} of (a) the top quark and (b) the Z boson in the SR 2j1b, for events with $O_{\mathrm{NN}} > 0.4$. The uncertainty band includes both the statistical and systematic uncertainties as obtained by the fit. The rightmost bin includes overflow events. The lower panels show the ratios of the data to the prediction.

10 Conclusion

The cross-section for tZq production, including non-resonant dilepton pairs with $m_{\ell^+\ell^-} > 30\,\text{GeV}$, is measured. The analysis uses $139\,\text{fb}^{-1}$ of proton-proton collision data collected by the ATLAS experiment at the LHC between 2015 and 2018 at a centre-of-mass energy of 13 TeV. The result of this measurement is 97 ± 13 (stat.) ± 7 (syst.) fb, assuming a top-quark mass of 172.5 GeV, corresponding to a total uncertainty of $\pm 14\%$. This result is in good agreement with the SM prediction of 102^{+5}_{-2} fb.

Acknowledgments

We thank CERN for the very successful operation of the LHC, as well as the support staff from our institutions without whom ATLAS could not be operated efficiently.

We acknowledge the support of ANPCyT, Argentina; YerPhI, Armenia; ARC, Australia; BMWFW and FWF, Austria; ANAS, Azerbaijan; SSTC, Belarus; CNPq and FAPESP, Brazil; NSERC, NRC and CFI, Canada; CERN; CONICYT, Chile; CAS, MOST and NSFC, China; COLCIENCIAS, Colombia; MSMT CR, MPO CR and VSC CR, Czech Republic; DNRF and DNSRC, Denmark; IN2P3-CNRS and CEA-DRF/IRFU, France; SRNSFG, Georgia; BMBF, HGF and MPG, Germany; GSRT, Greece; RGC and Hong Kong SAR, China; ISF and Benoziyo Center, Israel; INFN, Italy; MEXT and JSPS, Japan; CNRST, Morocco; NWO, Netherlands; RCN, Norway; MNiSW and NCN, Poland; FCT, Portugal; MNE/IFA, Romania; MES of Russia and NRC KI, Russia Federation; JINR; MESTD, Serbia; MSSR, Slovakia; ARRS and MIZŠ, Slovenia; DST/NRF, South Africa; MINECO, Spain; SRC and Wallenberg Foundation, Sweden; SERI, SNSF and Cantons of Bern and Geneva, Switzerland; MOST, Taiwan; TAEK, Turkey; STFC, United Kingdom; DOE and NSF, United States of America. In addition, individual groups and members have received support from BCKDF, CANARIE, Compute Canada and CRC, Canada; ERC, ERDF, Horizon 2020, Marie Skłodowska-Curie Actions and COST, European Union; Investissements d'Avenir Labex, Investissements d'Avenir Idex and ANR, France; DFG and AvH Foundation, Germany; Herakleitos, Thales and Aristeia programmes co-financed by EU-ESF and the Greek NSRF, Greece; BSF-NSF and GIF, Israel; CERCA Programme Generalitat de Catalunya and PROMETEO Programme Generalitat Valenciana, Spain; Göran Gustafssons Stiftelse, Sweden; The Royal Society and Leverhulme Trust, United Kingdom.

The crucial computing support from all WLCG partners is acknowledged gratefully, in particular from CERN, the ATLAS Tier-1 facilities at TRIUMF (Canada), NDGF (Denmark, Norway, Sweden), CC-IN2P3 (France), KIT/GridKA (Germany), INFN-CNAF (Italy), NL-T1 (Netherlands), PIC (Spain), ASGC (Taiwan), RAL (UK) and BNL (USA), the Tier-2 facilities worldwide and large non-WLCG resource providers. Major contributors of computing resources are listed in ref. [79].

JHEP07(2020)124

A Validation regions

The normalisation and modelling of the four main backgrounds are constrained using CRs. Additional diboson and $t\bar{t}$ +$t\bar{t}V$ validation regions (VRs) are used to confirm the goodness of the background modelling. These VRs are defined so as to be as close as possible to both the SRs and CRs.

The diboson VRs are defined using the same selection as the SRs except that a "loose" b-tag requirement (indicated as *1Lb* in the region name) is imposed that has a b-jet selection efficiency in the range 85%–70%. The $t\bar{t}$ + $t\bar{t}V$ VRs are defined using the same selection as the SRs except that the OSSF invariant mass requirement is inverted.

The NN training from each SR is applied to the corresponding VRs. Distributions of the O_{NN} in the various VRs are shown in figure 6. Any variables used in the NN training that are undefined in the VRs (e.g. due to missing jets) are replaced by a dummy value such that the variable is not used by NeuroBayes during the evaluation. This is also valid for the variables that have a different range compared to the one that was used in the training, such as the b-tagging score.

JHEP07(2020)124

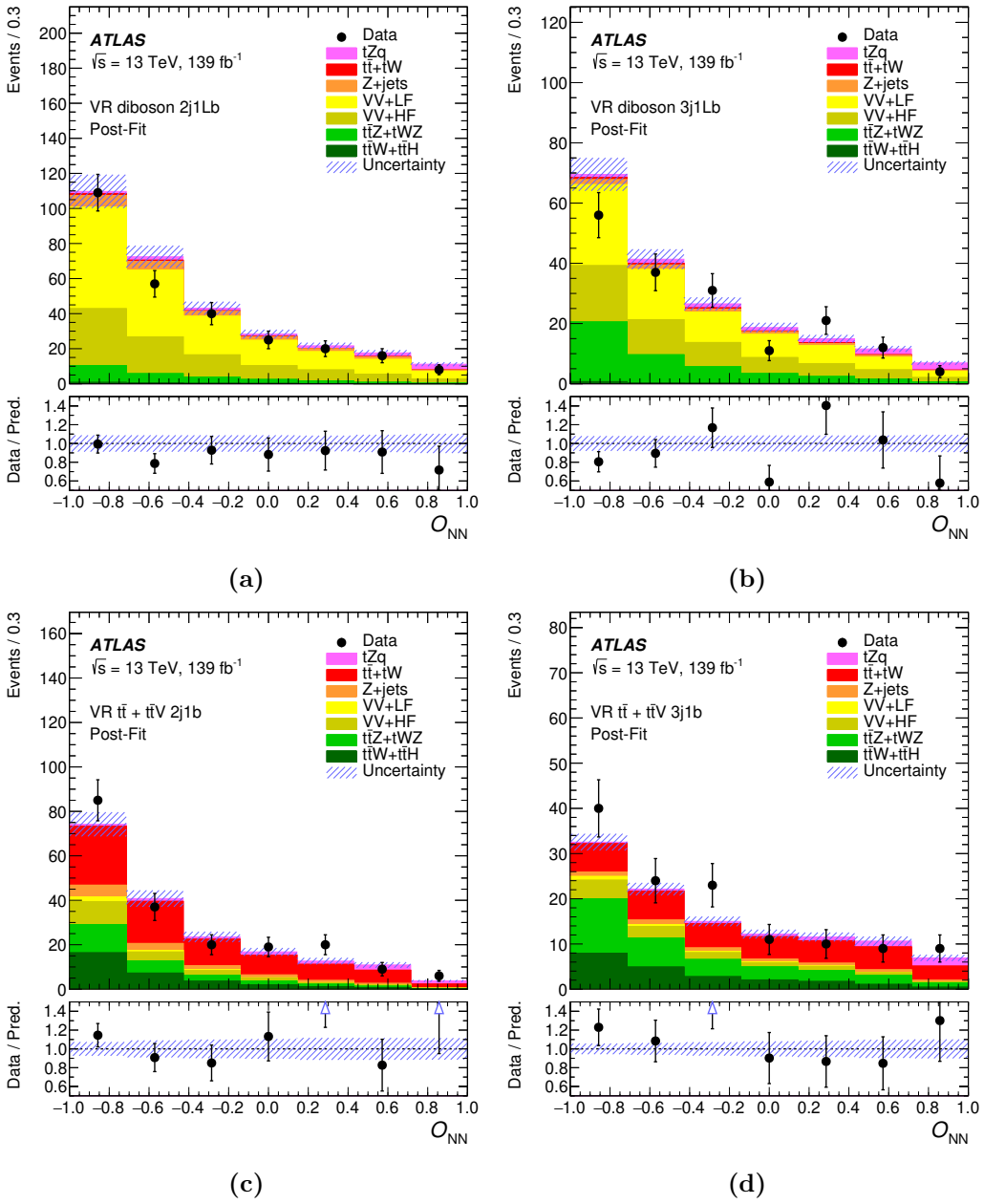

Figure 6. Comparison between data and prediction ("Pred.") after the fit to data ("Post-Fit") under the signal-plus-background hypothesis for the O_{NN} distributions in the VRs (a) diboson 2j1Lb, (b) diboson 3j1Lb, (c) $t\bar{t}$ + $t\bar{t}V$ 2j1b and (d) $t\bar{t}$ + $t\bar{t}V$ 3j1b. The uncertainty band includes both the statistical and systematic uncertainties as obtained by the fit. The lower panels show the ratios of the data to the prediction. The open triangles indicate points that are outside the vertical range of the figure.

JHEP07(2020)124

Open Access. This article is distributed under the terms of the Creative Commons Attribution License (CC-BY 4.0), which permits any use, distribution and reproduction in any medium, provided the original author(s) and source are credited.

References

[1] ATLAS collaboration, *Measurement of the production cross-section of a single top quark in association with a Z boson in proton-R-proton collisions at 13 TeV with the ATLAS detector*, *Phys. Lett. B* **780** (2018) 557 [arXiv:1710.03659] [INSPIRE].

[2] CMS collaboration, *Observation of Single Top Quark Production in Association with a Z Boson in Proton-Proton Collisions at* $\sqrt{s} = 13$ *TeV*, *Phys. Rev. Lett.* **122** (2019) 132003 [arXiv:1812.05900] [INSPIRE].

[3] C. Degrande, F. Maltoni, K. Mimasu, E. Vryonidou and C. Zhang, *Single-top associated production with a Z or H boson at the LHC: the SMEFT interpretation*, *JHEP* **10** (2018) 005 [arXiv:1804.07773] [INSPIRE].

[4] ATLAS collaboration, *The ATLAS Experiment at the CERN Large Hadron Collider*, 2008 *JINST* **3** S08003 [INSPIRE].

[5] ATLAS collaboration, *ATLAS Insertable B-Layer Technical Design Report*, ATLAS-TDR-19 (2010), Addendum: ATLAS-TDR-19-ADD-1 (2012).

[6] ATLAS IBL collaboration, *Production and Integration of the ATLAS Insertable B-Layer*, 2018 *JINST* **13** T05008 [arXiv:1803.00844] [INSPIRE].

[7] ATLAS collaboration, *Performance of the ATLAS Trigger System in 2015*, *Eur. Phys. J. C* **77** (2017) 317 [arXiv:1611.09661] [INSPIRE].

[8] ATLAS collaboration, *ATLAS data quality operations and performance for 2015–2018 data-taking*, 2020 *JINST* **15** P04003 [arXiv:1911.04632] [INSPIRE].

[9] ATLAS collaboration, *Performance of electron and photon triggers in ATLAS during LHC Run 2*, *Eur. Phys. J. C* **80** (2020) 47 [arXiv:1909.00761] [INSPIRE].

[10] ATLAS collaboration, *2015 start-up trigger menu and initial performance assessment of the ATLAS trigger using Run-2 data*, ATL-DAQ-PUB-2016-001 (2016).

[11] ATLAS collaboration, *Trigger Menu in 2016*, ATL-DAQ-PUB-2017-001 (2017).

[12] ATLAS collaboration, *Trigger Menu in 2017*, ATL-DAQ-PUB-2018-002 (2018).

[13] ATLAS collaboration, *Trigger menu in 2018*, ATL-DAQ-PUB-2019-001 (2019).

[14] GEANT4 collaboration, *GEANT4 — a simulation toolkit*, *Nucl. Instrum. Meth. A* **506** (2003) 250 [INSPIRE].

[15] ATLAS collaboration, *The ATLAS Simulation Infrastructure*, *Eur. Phys. J. C* **70** (2010) 823 [arXiv:1005.4568] [INSPIRE].

[16] T. Sjöstrand, S. Mrenna and P.Z. Skands, *A Brief Introduction to PYTHIA 8.1*, *Comput. Phys. Commun.* **178** (2008) 852 [arXiv:0710.3820] [INSPIRE].

[17] ATLAS collaboration, *The PYTHIA 8 A3 tune description of ATLAS minimum bias and inelastic measurements incorporating the Donnachie-Landshoff diffractive model*, ATL-PHYS-PUB-2016-017 (2016).

JHEP07(2020)124

[18] R.D. Ball et al., *Parton distributions with LHC data*, *Nucl. Phys. B* **867** (2013) 244 [arXiv:1207.1303] [INSPIRE].

[19] J. Alwall et al., *The automated computation of tree-level and next-to-leading order differential cross sections and their matching to parton shower simulations*, *JHEP* **07** (2014) 079 [arXiv:1405.0301] [INSPIRE].

[20] NNPDF collaboration, *Parton distributions for the LHC Run II*, *JHEP* **04** (2015) 040 [arXiv:1410.8849] [INSPIRE].

[21] R. Frederix, E. Re and P. Torrielli, *Single-top t-channel hadroproduction in the four-flavour scheme with POWHEG and aMC@NLO*, *JHEP* **09** (2012) 130 [arXiv:1207.5391] [INSPIRE].

[22] T. Sjöstrand et al., *An introduction to PYTHIA 8.2*, *Comput. Phys. Commun.* **191** (2015) 159 [arXiv:1410.3012] [INSPIRE].

[23] ATLAS collaboration, *ATLAS Pythia-8 tunes to 7 TeV data*, ATL-PHYS-PUB-2014-021 (2014).

[24] J. Butterworth et al., *PDF4LHC recommendations for LHC Run II*, *J. Phys. G* **43** (2016) 023001 [arXiv:1510.03865] [INSPIRE].

[25] P. Nason, *A new method for combining NLO QCD with shower Monte Carlo algorithms*, *JHEP* **11** (2004) 040 [hep-ph/0409146] [INSPIRE].

[26] S. Frixione, P. Nason and C. Oleari, *Matching NLO QCD computations with Parton Shower simulations: the POWHEG method*, *JHEP* **11** (2007) 070 [arXiv:0709.2092] [INSPIRE].

[27] S. Alioli, P. Nason, C. Oleari and E. Re, *A general framework for implementing NLO calculations in shower Monte Carlo programs: the POWHEG BOX*, *JHEP* **06** (2010) 043 [arXiv:1002.2581] [INSPIRE].

[28] S. Frixione, P. Nason and G. Ridolfi, *A positive-weight next-to-leading-order Monte Carlo for heavy flavour hadroproduction*, *JHEP* **09** (2007) 126 [arXiv:0707.3088] [INSPIRE].

[29] H.B. Hartanto, B. Jager, L. Reina and D. Wackeroth, *Higgs boson production in association with top quarks in the POWHEG BOX*, *Phys. Rev. D* **91** (2015) 094003 [arXiv:1501.04498] [INSPIRE].

[30] ATLAS collaboration, *Studies on top-quark Monte Carlo modelling for Top2016*, ATL-PHYS-PUB-2016-020 (2016).

[31] ATLAS collaboration, *Improvements in $t\bar{t}$ modelling using NLO+PS Monte Carlo generators for Run2*, ATL-PHYS-PUB-2018-009 (2018).

[32] ATLAS collaboration, *Studies on top-quark Monte Carlo modelling with Sherpa and MG5_aMC@NLO*, ATL-PHYS-PUB-2017-007 (2017).

[33] M. Bahr et al., *HERWIG++ Physics and Manual*, *Eur. Phys. J. C* **58** (2008) 639 [arXiv:0803.0883] [INSPIRE].

[34] J. Bellm et al., *HERWIG 7.0/HERWIG++ 3.0 release note*, *Eur. Phys. J. C* **76** (2016) 196 [arXiv:1512.01178] [INSPIRE].

[35] L.A. Harland-Lang, A.D. Martin, P. Motylinski and R.S. Thorne, *Parton distributions in the LHC era: MMHT 2014 PDFs*, *Eur. Phys. J. C* **75** (2015) 204 [arXiv:1412.3989] [INSPIRE].

[36] T. Gleisberg et al., *Event generation with SHERPA 1.1*, *JHEP* **02** (2009) 007 [arXiv:0811.4622] [INSPIRE].

JHEP07(2020)124

[37] E. Re, *Single-top Wt-channel production matched with parton showers using the POWHEG method*, *Eur. Phys. J. C* **71** (2011) 1547 [arXiv:1009.2450] [INSPIRE].

[38] S. Frixione, E. Laenen, P. Motylinski, B.R. Webber and C.D. White, *Single-top hadroproduction in association with a W boson*, *JHEP* **07** (2008) 029 [arXiv:0805.3067] [INSPIRE].

[39] F. Demartin, B. Maier, F. Maltoni, K. Mawatari and M. Zaro, *tWH associated production at the LHC*, *Eur. Phys. J. C* **77** (2017) 34 [arXiv:1607.05862] [INSPIRE].

[40] T. Gleisberg and S. Hoeche, *Comix, a new matrix element generator*, *JHEP* **12** (2008) 039 [arXiv:0808.3674] [INSPIRE].

[41] S. Schumann and F. Krauss, *A parton shower algorithm based on Catani-Seymour dipole factorisation*, *JHEP* **03** (2008) 038 [arXiv:0709.1027] [INSPIRE].

[42] S. Hoeche, F. Krauss, M. Schonherr and F. Siegert, *A critical appraisal of NLO+PS matching methods*, *JHEP* **09** (2012) 049 [arXiv:1111.1220] [INSPIRE].

[43] S. Hoeche, F. Krauss, M. Schonherr and F. Siegert, *QCD matrix elements + parton showers: The NLO case*, *JHEP* **04** (2013) 027 [arXiv:1207.5030] [INSPIRE].

[44] S. Catani, F. Krauss, R. Kuhn and B.R. Webber, *QCD matrix elements + parton showers*, *JHEP* **11** (2001) 063 [hep-ph/0109231] [INSPIRE].

[45] S. Hoeche, F. Krauss, S. Schumann and F. Siegert, *QCD matrix elements and truncated showers*, *JHEP* **05** (2009) 053 [arXiv:0903.1219] [INSPIRE].

[46] F. Cascioli, P. Maierhofer and S. Pozzorini, *Scattering Amplitudes with Open Loops*, *Phys. Rev. Lett.* **108** (2012) 111601 [arXiv:1111.5206] [INSPIRE].

[47] A. Denner, S. Dittmaier and L. Hofer, *Collier: a fortran-based Complex One-Loop LIbrary in Extended Regularizations*, *Comput. Phys. Commun.* **212** (2017) 220 [arXiv:1604.06792] [INSPIRE].

[48] P. Nason and G. Zanderighi, W^+W^-, WZ *and* ZZ *production in the POWHEG-BOX-V2*, *Eur. Phys. J. C* **74** (2014) 2702 [arXiv:1311.1365] [INSPIRE].

[49] H.-L. Lai et al., *New parton distributions for collider physics*, *Phys. Rev. D* **82** (2010) 074024 [arXiv:1007.2241] [INSPIRE].

[50] ATLAS collaboration, *Measurement of the* Z/γ^* *boson transverse momentum distribution in pp collisions at* $\sqrt{s} = 7$ *TeV with the ATLAS detector*, *JHEP* **09** (2014) 145 [arXiv:1406.3660] [INSPIRE].

[51] J. Pumplin, D.R. Stump, J. Huston, H.L. Lai, P.M. Nadolsky and W.K. Tung, *New generation of parton distributions with uncertainties from global QCD analysis*, *JHEP* **07** (2002) 012 [hep-ph/0201195] [INSPIRE].

[52] *Vertex Reconstruction Performance of the ATLAS Detector at* $\sqrt{s} = 13$ *TeV*, ATL-PHYS-PUB-2015-026 (2015).

[53] ATLAS collaboration, *Electron and photon performance measurements with the ATLAS detector using the 2015–2017 LHC proton-proton collision data*, 2019 *JINST* **14** P12006 [arXiv:1908.00005] [INSPIRE].

[54] ATLAS collaboration, *Muon reconstruction performance of the ATLAS detector in proton–proton collision data at* $\sqrt{s} = 13$ *TeV*, *Eur. Phys. J. C* **76** (2016) 292 [arXiv:1603.05598] [INSPIRE].

JHEP07(2020)124

[55] ATLAS collaboration, *Topological cell clustering in the ATLAS calorimeters and its performance in LHC Run 1*, *Eur. Phys. J. C* **77** (2017) 490 [arXiv:1603.02934] [INSPIRE].

[56] M. Cacciari and G.P. Salam, *Dispelling the N^3 myth for the k_t jet-finder*, *Phys. Lett. B* **641** (2006) 57 [hep-ph/0512210] [INSPIRE].

[57] M. Cacciari, G.P. Salam and G. Soyez, *The anti-k_t jet clustering algorithm*, *JHEP* **04** (2008) 063 [arXiv:0802.1189] [INSPIRE].

[58] M. Cacciari, G.P. Salam and G. Soyez, *FastJet User Manual*, *Eur. Phys. J. C* **72** (2012) 1896 [arXiv:1111.6097] [INSPIRE].

[59] ATLAS collaboration, *Jet energy scale measurements and their systematic uncertainties in proton-proton collisions at $\sqrt{s} = 13$ TeV with the ATLAS detector*, *Phys. Rev. D* **96** (2017) 072002 [arXiv:1703.09665] [INSPIRE].

[60] ATLAS collaboration, *Performance of pile-up mitigation techniques for jets in pp collisions at $\sqrt{s} = 8$ TeV using the ATLAS detector*, *Eur. Phys. J. C* **76** (2016) 581 [arXiv:1510.03823] [INSPIRE].

[61] ATLAS collaboration, *Identification and rejection of pile-up jets at high pseudorapidity with the ATLAS detector*, *Eur. Phys. J. C* **77** (2017) 580 [*Erratum ibid.* **77** (2017) 712] [arXiv:1705.02211] [INSPIRE].

[62] ATLAS collaboration, *ATLAS b-jet identification performance and efficiency measurement with $t\bar{t}$ events in pp collisions at $\sqrt{s} = 13$ TeV*, *Eur. Phys. J. C* **79** (2019) 970 [arXiv:1907.05120] [INSPIRE].

[63] ATLAS collaboration, *Optimisation and performance studies of the ATLAS b-tagging algorithms for the 2017-18 LHC run*, ATL-PHYS-PUB-2017-013 (2017).

[64] ATLAS collaboration, *Measurement of b-tagging Efficiency of c-jets in $t\bar{t}$ Events Using a Likelihood Approach with the ATLAS Detector*, ATLAS-CONF-2018-001 (2018).

[65] ATLAS collaboration, *Calibration of light-flavour b-jet mistagging rates using ATLAS proton-proton collision data at $\sqrt{s} = 13$ TeV*, ATLAS-CONF-2018-006 (2018).

[66] ATLAS collaboration, *Performance of missing transverse momentum reconstruction with the ATLAS detector using proton-proton collisions at $\sqrt{s} = 13$ TeV*, *Eur. Phys. J. C* **78** (2018) 903 [arXiv:1802.08168] [INSPIRE].

[67] ATLAS collaboration, *Search for FCNC single top-quark production at $\sqrt{s} = 7$ TeV with the ATLAS detector*, *Phys. Lett. B* **712** (2012) 351 [arXiv:1203.0529] [INSPIRE].

[68] A. Kulesza, L. Motyka, T. Stebel and V. Theeuwes, *Soft gluon resummation for associated $t\bar{t}H$ production at the LHC*, *JHEP* **03** (2016) 065 [arXiv:1509.02780] [INSPIRE].

[69] M. Feindt, *A Neural Bayesian Estimator for Conditional Probability Densities*, physics/0402093 [INSPIRE].

[70] M. Feindt and U. Kerzel, *The NeuroBayes neural network package*, *Nucl. Instrum. Meth. A* **559** (2006) 190 [INSPIRE].

[71] ATLAS collaboration, *Measurement of the t-channel single top-quark production cross section in pp collisions at $\sqrt{s} = 7$ TeV with the ATLAS detector*, *Phys. Lett. B* **717** (2012) 330 [arXiv:1205.3130] [INSPIRE].

[72] ATLAS collaboration, *Simulation of top quark production for the ATLAS experiment at $\sqrt{s} = 13$ TeV*, ATL-PHYS-PUB-2016-004 (2016).

JHEP07(2020)124

[73] D. de Florian et al., *Handbook of LHC Higgs Cross Sections: 4. Deciphering the Nature of the Higgs Sector*, arXiv:1610.07922 [INSPIRE].

[74] ATLAS collaboration, *Measurement of $W^{\pm}Z$ production cross sections and gauge boson polarisation in pp collisions at $\sqrt{s} = 13$ TeV with the ATLAS detector*, *Eur. Phys. J. C* **79** (2019) 535 [arXiv:1902.05759] [INSPIRE].

[75] ATLAS collaboration, *Evidence for the $H \to b\bar{b}$ decay with the ATLAS detector*, *JHEP* **12** (2017) 024 [arXiv:1708.03299] [INSPIRE].

[76] ATLAS collaboration, *Luminosity determination in pp collisions at $\sqrt{s} = 13$ TeV using the ATLAS detector at the LHC*, ATLAS-CONF-2019-021(2019).

[77] G. Avoni et al., *The new LUCID-2 detector for luminosity measurement and monitoring in ATLAS*, 2018 *JINST* **13** P07017 [INSPIRE].

[78] G. Cowan, K. Cranmer, E. Gross and O. Vitells, *Asymptotic formulae for likelihood-based tests of new physics*, *Eur. Phys. J. C* **71** (2011) 1554 [*Erratum ibid.* **73** (2013) 2501] [arXiv:1007.1727] [INSPIRE].

[79] ATLAS collaboration, *ATLAS Computing Acknowledgements*, ATL-GEN-PUB-2016-002 (2016).

JHEP07(2020)124

The ATLAS collaboration

G. Aad[102], B. Abbott[129], D.C. Abbott[103], A. Abed Abud[36], K. Abeling[53], D.K. Abhayasinghe[94], S.H. Abidi[167], O.S. AbouZeid[40], N.L. Abraham[156], H. Abramowicz[161], H. Abreu[160], Y. Abulaiti[6], B.S. Acharya[67a,67b,n], B. Achkar[53], S. Adachi[163], L. Adam[100], C. Adam Bourdarios[5], L. Adamczyk[84a], L. Adamek[167], J. Adelman[121], M. Adersberger[114], A. Adiguzel[12c], S. Adorni[54], T. Adye[144], A.A. Affolder[146], Y. Afik[160], C. Agapopoulou[65], M.N. Agaras[38], A. Aggarwal[119], C. Agheorghiesei[27c], J.A. Aguilar-Saavedra[140f,140a,af], F. Ahmadov[80], W.S. Ahmed[104], X. Ai[18], G. Aielli[74a,74b], S. Akatsuka[86], T.P.A. Åkesson[97], E. Akilli[54], A.V. Akimov[111], K. Al Khoury[65], G.L. Alberghi[23b,23a], J. Albert[176], M.J. Alconada Verzini[161], S. Alderweireldt[36], M. Aleksa[36], I.N. Aleksandrov[80], C. Alexa[27b], T. Alexopoulos[10], A. Alfonsi[120], F. Alfonsi[23b,23a], M. Alhroob[129], B. Ali[142], M. Aliev[166], G. Alimonti[69a], C. Allaire[65], B.M.M. Allbrooke[156], B.W. Allen[132], P.P. Allport[21], A. Aloisio[70a,70b], F. Alonso[89], C. Alpigiani[148], A.A. Alshehri[57], E. Alunno Camelia[74a,74b], M. Alvarez Estevez[99], M.G. Alviggi[70a,70b], Y. Amaral Coutinho[81b], A. Ambler[104], L. Ambroz[135], C. Amelung[26], D. Amidei[106], S.P. Amor Dos Santos[140a], S. Amoroso[46], C.S. Amrouche[54], F. An[79], C. Anastopoulos[149], N. Andari[145], T. Andeen[11], C.F. Anders[61b], J.K. Anders[20], A. Andreazza[69a,69b], V. Andrei[61a], C.R. Anelli[176], S. Angelidakis[38], A. Angerami[39], A.V. Anisenkov[122b,122a], A. Annovi[72a], C. Antel[54], M.T. Anthony[149], E. Antipov[130], M. Antonelli[51], D.J.A. Antrim[171], F. Anulli[73a], M. Aoki[82], J.A. Aparisi Pozo[174], L. Aperio Bella[15a], J.P. Araque[140a], V. Araujo Ferraz[81b], R. Araujo Pereira[81b], C. Arcangeletti[51], A.T.H. Arce[49], F.A. Arduh[89], J-F. Arguin[110], S. Argyropoulos[52], J.-H. Arling[46], A.J. Armbruster[36], A. Armstrong[171], O. Arnaez[167], H. Arnold[120], Z.P. Arrubarrena Tame[114], G. Artoni[135], S. Artz[100], S. Asai[163], T. Asawatavonvanich[165], N. Asbah[59], E.M. Asimakopoulou[172], L. Asquith[156], J. Assahsah[35d], K. Assamagan[29], R. Astalos[28a], R.J. Atkin[33a], M. Atkinson[173], N.B. Atlay[19], H. Atmani[65], K. Augsten[142], G. Avolio[36], M.K. Ayoub[15a], G. Azuelos[110,ap], H. Bachacou[145], K. Bachas[68a,68b], M. Backes[135], F. Backman[45a,45b], P. Bagnaia[73a,73b], M. Bahmani[85], H. Bahrasemani[152], A.J. Bailey[174], V.R. Bailey[173], J.T. Baines[144], C. Bakalis[10], O.K. Baker[183], P.J. Bakker[120], D. Bakshi Gupta[8], S. Balaji[157], E.M. Baldin[122b,122a], P. Balek[180], F. Balli[145], W.K. Balunas[135], J. Balz[100], E. Banas[85], A. Bandyopadhyay[24], Sw. Banerjee[181,i], A.A.E. Bannoura[182], L. Barak[161], W.M. Barbe[38], E.L. Barberio[105], D. Barberis[55b,55a], M. Barbero[102], G. Barbour[95], T. Barillari[115], M-S. Barisits[36], J. Barkeloo[132], T. Barklow[153], R. Barnea[160], B.M. Barnett[144], R.M. Barnett[18], Z. Barnovska-Blenessy[60a], A. Baroncelli[60a], G. Barone[29], A.J. Barr[135], L. Barranco Navarro[45a,45b], F. Barreiro[99], J. Barreiro Guimarães da Costa[15a], S. Barsov[138], R. Bartoldus[153], G. Bartolini[102], A.E. Barton[90], P. Bartos[28a], A. Basalaev[46], A. Basan[100], A. Bassalat[65,al], M.J. Basso[167], R.L. Bates[57], S. Batlamous[35e], J.R. Batley[32], B. Batool[151], M. Battaglia[146], M. Bauce[73a,73b], F. Bauer[145], K.T. Bauer[171], H.S. Bawa[31], J.B. Beacham[49], T. Beau[136], P.H. Beauchemin[170], F. Becherer[52], P. Bechtle[24], H.C. Beck[53], H.P. Beck[20,r], K. Becker[178], C. Becot[46], A. Beddall[12d], A.J. Beddall[12a], V.A. Bednyakov[80], M. Bedognetti[120], C.P. Bee[155], T.A. Beermann[182], M. Begalli[81b], M. Begel[29], A. Behera[155], J.K. Behr[46], F. Beisiegel[24], A.S. Bell[95], G. Bella[161], L. Bellagamba[23b], A. Bellerive[34], P. Bellos[9], K. Beloborodov[122b,122a], K. Belotskiy[112], N.L. Belyaev[112], D. Benchekroun[35a], N. Benekos[10], Y. Benhammou[161], D.P. Benjamin[6], M. Benoit[54], J.R. Bensinger[26], S. Bentvelsen[120], L. Beresford[135], M. Beretta[51], D. Berge[19], E. Bergeaas Kuutmann[172], N. Berger[5], B. Bergmann[142], L.J. Bergsten[26], J. Beringer[18], S. Berlendis[7], G. Bernardi[136], C. Bernius[153], F.U. Bernlochner[24], T. Berry[94], P. Berta[100], C. Bertella[15a], I.A. Bertram[90], O. Bessidskaia Bylund[182], N. Besson[145], A. Bethani[101], S. Bethke[115], A. Betti[42], A.J. Bevan[93], J. Beyer[115], D.S. Bhattacharya[177], P. Bhattarai[26], R. Bi[139], R.M. Bianchi[139], O. Biebel[114], D. Biedermann[19], R. Bielski[36], K. Bierwagen[100],

JHEP07(2020)124

N.V. Biesuz[72a,72b], M. Biglietti[75a], T.R.V. Billoud[110], M. Bindi[53], A. Bingul[12d], C. Bini[73a,73b], S. Biondi[23b,23a], M. Birman[180], T. Bisanz[53], J.P. Biswal[3], D. Biswas[181,i], A. Bitadze[101], C. Bittrich[48], K. Bjørke[134], T. Blazek[28a], I. Bloch[46], C. Blocker[26], A. Blue[57], U. Blumenschein[93], G.J. Bobbink[120], V.S. Bobrovnikov[122b,122a], S.S. Bocchetta[97], A. Bocci[49], D. Boerner[46], D. Bogavac[14], A.G. Bogdanchikov[122b,122a], C. Bohm[45a], V. Boisvert[94], P. Bokan[53,172], T. Bold[84a], A.E. Bolz[61b], M. Bomben[136], M. Bona[93], J.S. Bonilla[132], M. Boonekamp[145], C.D. Booth[94], H.M. Borecka-Bielska[91], L.S. Borgna[95], A. Borisov[123], G. Borissov[90], J. Bortfeldt[36], D. Bortoletto[135], D. Boscherini[23b], M. Bosman[14], J.D. Bossio Sola[104], K. Bouaouda[35a], J. Boudreau[139], E.V. Bouhova-Thacker[90], D. Boumediene[38], S.K. Boutle[57], A. Boveia[127], J. Boyd[36], D. Boye[33c,am], I.R. Boyko[80], A.J. Bozson[94], J. Bracinik[21], N. Brahimi[102], G. Brandt[182], O. Brandt[32], F. Braren[46], B. Brau[103], J.E. Brau[132], W.D. Breaden Madden[57], K. Brendlinger[46], L. Brenner[46], R. Brenner[172], S. Bressler[180], B. Brickwedde[100], D.L. Briglin[21], D. Britton[57], D. Britzger[115], I. Brock[24], R. Brock[107], G. Brooijmans[39], W.K. Brooks[147d], E. Brost[29], J.H Broughton[21], P.A. Bruckman de Renstrom[85], D. Bruncko[28b], A. Bruni[23b], G. Bruni[23b], L.S. Bruni[120], S. Bruno[74a,74b], M. Bruschi[23b], N. Bruscino[73a,73b], P. Bryant[37], L. Bryngemark[97], T. Buanes[17], Q. Buat[36], P. Buchholz[151], A.G. Buckley[57], I.A. Budagov[80], M.K. Bugge[134], F. Bührer[52], O. Bulekov[112], T.J. Burch[121], S. Burdin[91], C.D. Burgard[120], A.M. Burger[130], B. Burghgrave[8], J.T.P. Burr[46], C.D. Burton[11], J.C. Burzynski[103], V. Büscher[100], E. Buschmann[53], P.J. Bussey[57], J.M. Butler[25], C.M. Buttar[57], J.M. Butterworth[95], P. Butti[36], W. Buttinger[36], C.J. Buxo Vazquez[107], A. Buzatu[158], A.R. Buzykaev[122b,122a], G. Cabras[23b,23a], S. Cabrera Urbán[174], D. Caforio[56], H. Cai[173], V.M.M. Cairo[153], O. Cakir[4a], N. Calace[36], P. Calafiura[18], A. Calandri[102], G. Calderini[136], P. Calfayan[66], G. Callea[57], L.P. Caloba[81b], A. Caltabiano[74a,74b], S. Calvente Lopez[99], D. Calvet[38], S. Calvet[38], T.P. Calvet[155], M. Calvetti[72a,72b], R. Camacho Toro[136], S. Camarda[36], D. Camarero Munoz[99], P. Camarri[74a,74b], D. Cameron[134], C. Camincher[36], S. Campana[36], M. Campanelli[95], A. Camplani[40], A. Campoverde[151], V. Canale[70a,70b], A. Canesse[104], M. Cano Bret[60c], J. Cantero[130], T. Cao[161], Y. Cao[173], M.D.M. Capeans Garrido[36], M. Capua[41b,41a], R. Cardarelli[74a], F. Cardillo[149], G. Carducci[41b,41a], I. Carli[143], T. Carli[36], G. Carlino[70a], B.T. Carlson[139], L. Carminati[69a,69b], R.M.D. Carney[153], S. Caron[119], E. Carquin[147d], S. Carrá[46], J.W.S. Carter[167], M.P. Casado[14,e], A.F. Casha[167], D.W. Casper[171], R. Castelijn[120], F.L. Castillo[174], L. Castillo Garcia[14], V. Castillo Gimenez[174], N.F. Castro[140a,140e], A. Catinaccio[36], J.R. Catmore[134], A. Cattai[36], V. Cavaliere[29], E. Cavallaro[14], M. Cavalli-Sforza[14], V. Cavasinni[72a,72b], E. Celebi[12b], L. Cerda Alberich[174], K. Cerny[131], A.S. Cerqueira[81a], A. Cerri[156], L. Cerrito[74a,74b], F. Cerutti[18], A. Cervelli[23b,23a], S.A. Cetin[12b], Z. Chadi[35a], D. Chakraborty[121], J. Chan[181], W.S. Chan[120], W.Y. Chan[91], J.D. Chapman[32], B. Chargeishvili[159b], D.G. Charlton[21], T.P. Charman[93], C.C. Chau[34], S. Che[127], S. Chekanov[6], S.V. Chekulaev[168a], G.A. Chelkov[80,aj], B. Chen[79], C. Chen[60a], C.H. Chen[79], H. Chen[29], J. Chen[60a], J. Chen[39], J. Chen[26], S. Chen[137], S.J. Chen[15c], X. Chen[15b], Y-H. Chen[46], H.C. Cheng[63a], H.J. Cheng[15a], A. Cheplakov[80], E. Cheremushkina[123], R. Cherkaoui El Moursli[35e], E. Cheu[7], K. Cheung[64], T.J.A. Chevalérias[145], L. Chevalier[145], V. Chiarella[51], G. Chiarelli[72a], G. Chiodini[68a], A.S. Chisholm[21], A. Chitan[27b], I. Chiu[163], Y.H. Chiu[176], M.V. Chizhov[80], K. Choi[11], A.R. Chomont[73a,73b], S. Chouridou[162], Y.S. Chow[120], M.C. Chu[63a], X. Chu[15a,15d], J. Chudoba[141], J.J. Chwastowski[85], L. Chytka[131], D. Cieri[115], K.M. Ciesla[85], D. Cinca[47], V. Cindro[92], I.A. Cioară[27b], A. Ciocio[18], F. Cirotto[70a,70b], Z.H. Citron[180,j], M. Citterio[69a], D.A. Ciubotaru[27b], B.M. Ciungu[167], A. Clark[54], M.R. Clark[39], P.J. Clark[50], C. Clement[45a,45b], Y. Coadou[102], M. Cobal[67a,67c], A. Coccaro[55b], J. Cochran[79], R. Coelho Lopes De Sa[103], H. Cohen[161], A.E.C. Coimbra[36], B. Cole[39], A.P. Colijn[120], J. Collot[58], P. Conde Muiño[140a,140h], S.H. Connell[33c], I.A. Connelly[57], S. Constantinescu[27b], F. Conventi[70a,aq], A.M. Cooper-Sarkar[135], F. Cormier[175], K.J.R. Cormier[167], L.D. Corpe[95], M. Corradi[73a,73b],

JHEP07(2020)124

E.E. Corrigan[97], F. Corriveau[104,ad], M.J. Costa[174], F. Costanza[5], D. Costanzo[149], G. Cowan[94], J.W. Cowley[32], J. Crane[101], K. Cranmer[125], S.J. Crawley[57], R.A. Creager[137], S. Crépé-Renaudin[58], F. Crescioli[136], M. Cristinziani[24], V. Croft[170], G. Crosetti[41b,41a], A. Cueto[5], T. Cuhadar Donszelmann[149], A.R. Cukierman[153], W.R. Cunningham[57], S. Czekierda[85], P. Czodrowski[36], M.J. Da Cunha Sargedas De Sousa[60b], J.V. Da Fonseca Pinto[81b], C. Da Via[101], W. Dabrowski[84a], F. Dachs[36], T. Dado[28a], S. Dahbi[33e], T. Dai[106], C. Dallapiccola[103], M. Dam[40], G. D'amen[29], V. D'Amico[75a,75b], J. Damp[100], J.R. Dandoy[137], M.F. Daneri[30], N.S. Dann[101], M. Danninger[152], V. Dao[36], G. Darbo[55b], O. Dartsi[5], A. Dattagupta[132], T. Daubney[46], S. D'Auria[69a,69b], C. David[168b], T. Davidek[143], D.R. Davis[49], I. Dawson[149], K. De[8], R. De Asmundis[70a], M. De Beurs[120], S. De Castro[23b,23a], S. De Cecco[73a,73b], N. De Groot[119], P. de Jong[120], H. De la Torre[107], A. De Maria[15c], D. De Pedis[73a], A. De Salvo[73a], U. De Sanctis[74a,74b], M. De Santis[74a,74b], A. De Santo[156], K. De Vasconcelos Corga[102], J.B. De Vivie De Regie[65], C. Debenedetti[146], D.V. Dedovich[80], A.M. Deiana[42], J. Del Peso[99], Y. Delabat Diaz[46], D. Delgove[65], F. Deliot[145,q], C.M. Delitzsch[7], M. Della Pietra[70a,70b], D. Della Volpe[54], A. Dell'Acqua[36], L. Dell'Asta[74a,74b], M. Delmastro[5], C. Delporte[65], P.A. Delsart[58], D.A. DeMarco[167], S. Demers[183], M. Demichev[80], G. Demontigny[110], S.P. Denisov[123], L. D'Eramo[136], D. Derendarz[85], J.E. Derkaoui[35d], F. Derue[136], P. Dervan[91], K. Desch[24], C. Deterre[46], K. Dette[167], C. Deutsch[24], M.R. Devesa[30], P.O. Deviveiros[36], F.A. Di Bello[54], A. Di Ciaccio[74a,74b], L. Di Ciaccio[5], W.K. Di Clemente[137], C. Di Donato[70a,70b], A. Di Girolamo[36], G. Di Gregorio[72a,72b], B. Di Micco[75a,75b], R. Di Nardo[75a,75b], K.F. Di Petrillo[59], R. Di Sipio[167], C. Diaconu[102], F.A. Dias[40], T. Dias Do Vale[140a], M.A. Diaz[147a], J. Dickinson[18], E.B. Diehl[106], J. Dietrich[19], S. Díez Cornell[46], A. Dimitrievska[18], W. Ding[15b], J. Dingfelder[24], F. Dittus[36], F. Djama[102], T. Djobava[159b], J.I. Djuvsland[17], M.A.B. Do Vale[81c], M. Dobre[27b], D. Dodsworth[26], C. Doglioni[97], J. Dolejsi[143], Z. Dolezal[143], M. Donadelli[81d], B. Dong[60c], J. Donini[38], A. D'onofrio[15c], M. D'Onofrio[91], J. Dopke[144], A. Doria[70a], M.T. Dova[89], A.T. Doyle[57], E. Drechsler[152], E. Dreyer[152], T. Dreyer[53], A.S. Drobac[170], D. Du[60b], Y. Duan[60b], F. Dubinin[111], M. Dubovsky[28a], A. Dubreuil[54], E. Duchovni[180], G. Duckeck[114], A. Ducourthial[136], O.A. Ducu[110], D. Duda[115], A. Dudarev[36], A.C. Dudder[100], E.M. Duffield[18], L. Duflot[65], M. Dührssen[36], C. Dülsen[182], M. Dumancic[180], A.E. Dumitriu[27b], A.K. Duncan[57], M. Dunford[61a], A. Duperrin[102], H. Duran Yildiz[4a], M. Düren[56], A. Durglishvili[159b], D. Duschinger[48], B. Dutta[46], D. Duvnjak[1], G.I. Dyckes[137], M. Dyndal[36], S. Dysch[101], B.S. Dziedzic[85], K.M. Ecker[115], M.G. Eggleston[49], T. Eifert[8], G. Eigen[17], K. Einsweiler[18], T. Ekelof[172], H. El Jarrari[35e], R. El Kosseifi[102], V. Ellajosyula[172], M. Ellert[172], F. Ellinghaus[182], A.A. Elliot[93], N. Ellis[36], J. Elmsheuser[29], M. Elsing[36], D. Emeliyanov[144], A. Emerman[39], Y. Enari[163], M.B. Epland[49], J. Erdmann[47], A. Ereditato[20], P.A. Erland[85], M. Errenst[36], M. Escalier[65], C. Escobar[174], O. Estrada Pastor[174], E. Etzion[161], H. Evans[66], A. Ezhilov[138], F. Fabbri[57], L. Fabbri[23b,23a], V. Fabiani[119], G. Facini[178], R.M. Faisca Rodrigues Pereira[140a], R.M. Fakhrutdinov[123], S. Falciano[73a], P.J. Falke[5], S. Falke[5], J. Faltova[143], Y. Fang[15a], Y. Fang[15a], G. Fanourakis[44], M. Fanti[69a,69b], M. Faraj[67a,67c,s], A. Farbin[8], A. Farilla[75a], E.M. Farina[71a,71b], T. Farooque[107], S.M. Farrington[50], P. Farthouat[36], F. Fassi[35e], P. Fassnacht[36], D. Fassouliotis[9], M. Faucci Giannelli[50], W.J. Fawcett[32], L. Fayard[65], O.L. Fedin[138,o], W. Fedorko[175], A. Fehr[20], M. Feickert[173], L. Feligioni[102], A. Fell[149], C. Feng[60b], M. Feng[49], M.J. Fenton[171], A.B. Fenyuk[123], S.W. Ferguson[43], J. Ferrando[46], A. Ferrante[173], A. Ferrari[172], P. Ferrari[120], R. Ferrari[71a], D.E. Ferreira de Lima[61b], A. Ferrer[174], D. Ferrere[54], C. Ferretti[106], F. Fiedler[100], A. Filipčič[92], F. Filthaut[119], K.D. Finelli[25], M.C.N. Fiolhais[140a,140c,a], L. Fiorini[174], F. Fischer[114], W.C. Fisher[107], I. Fleck[151], P. Fleischmann[106], T. Flick[182], B.M. Flierl[114], L. Flores[137], L.R. Flores Castillo[63a], F.M. Follega[76a,76b], N. Fomin[17], J.H. Foo[167], G.T. Forcolin[76a,76b], A. Formica[145], F.A. Förster[14], A.C. Forti[101], A.G. Foster[21], M.G. Foti[135],

JHEP07(2020)124

D. Fournier[65], H. Fox[90], P. Francavilla[72a,72b], S. Francescato[73a,73b], M. Franchini[23b,23a], S. Franchino[61a], D. Francis[36], L. Franconi[20], M. Franklin[59], A.N. Fray[93], P.M. Freeman[21], B. Freund[110], W.S. Freund[81b], E.M. Freundlich[47], D.C. Frizzell[129], D. Froidevaux[36], J.A. Frost[135], C. Fukunaga[164], E. Fullana Torregrosa[174], T. Fusayasu[116], J. Fuster[174], A. Gabrielli[23b,23a], A. Gabrielli[18], S. Gadatsch[54], P. Gadow[115], G. Gagliardi[55b,55a], L.G. Gagnon[110], B. Galhardo[140a], G.E. Gallardo[135], E.J. Gallas[135], B.J. Gallop[144], G. Galster[40], R. Gamboa Goni[93], K.K. Gan[127], S. Ganguly[180], J. Gao[60a], Y. Gao[50], Y.S. Gao[31,l], C. García[174], J.E. García Navarro[174], J.A. García Pascual[15a], C. Garcia-Argos[52], M. Garcia-Sciveres[18], R.W. Gardner[37], N. Garelli[153], S. Gargiulo[52], C.A. Garner[167], V. Garonne[134], S.J. Gasiorowski[148], P. Gaspar[81b], A. Gaudiello[55b,55a], G. Gaudio[71a], I.L. Gavrilenko[111], A. Gavrilyuk[124], C. Gay[175], G. Gaycken[46], E.N. Gazis[10], A.A. Geanta[27b], C.M. Gee[146], C.N.P. Gee[144], J. Geisen[97], M. Geisen[100], C. Gemme[55b], M.H. Genest[58], C. Geng[106], S. Gentile[73a,73b], S. George[94], T. Geralis[44], L.O. Gerlach[53], P. Gessinger-Befurt[100], G. Gessner[47], S. Ghasemi[151], M. Ghasemi Bostanabad[176], M. Ghneimat[151], A. Ghosh[65], A. Ghosh[78], B. Giacobbe[23b], S. Giagu[73a,73b], N. Giangiacomi[23b,23a], P. Giannetti[72a], A. Giannini[70a,70b], G. Giannini[14], S.M. Gibson[94], M. Gignac[146], D. Gillberg[34], G. Gilles[182], D.M. Gingrich[3,ap], M.P. Giordani[67a,67c], P.F. Giraud[145], G. Giugliarelli[67a,67c], D. Giugni[69a], F. Giuli[74a,74b], S. Gkaitatzis[162], I. Gkialas[9,g], E.L. Gkougkousis[14], P. Gkountoumis[10], L.K. Gladilin[113], C. Glasman[99], J. Glatzer[14], P.C.F. Glaysher[46], A. Glazov[46], G.R. Gledhill[132], M. Goblirsch-Kolb[26], D. Godin[110], S. Goldfarb[105], T. Golling[54], D. Golubkov[123], A. Gomes[140a,140b], R. Goncalves Gama[53], R. Gonçalo[140a], G. Gonella[132], L. Gonella[21], A. Gongadze[80], F. Gonnella[21], J.L. Gonski[39], S. González de la Hoz[174], S. Gonzalez Fernandez[14], S. Gonzalez-Sevilla[54], G.R. Gonzalvo Rodriguez[174], L. Goossens[36], N.A. Gorasia[21], P.A. Gorbounov[124], H.A. Gordon[29], B. Gorini[36], E. Gorini[68a,68b], A. Gorišek[92], A.T. Goshaw[49], M.I. Gostkin[80], C.A. Gottardo[119], M. Gouighri[35b], A.G. Goussiou[148], N. Govender[33c], C. Goy[5], E. Gozani[160], I. Grabowska-Bold[84a], E.C. Graham[91], J. Gramling[171], E. Gramstad[134], S. Grancagnolo[19], M. Grandi[156], V. Gratchev[138], P.M. Gravila[27f], F.G. Gravili[68a,68b], C. Gray[57], H.M. Gray[18], C. Grefe[24], K. Gregersen[97], I.M. Gregor[46], P. Grenier[153], K. Grevtsov[46], C. Grieco[14], N.A. Grieser[129], A.A. Grillo[146], K. Grimm[31,k], S. Grinstein[14,y], J.-F. Grivaz[65], S. Groh[100], E. Gross[180], J. Grosse-Knetter[53], Z.J. Grout[95], C. Grud[106], A. Grummer[118], L. Guan[106], W. Guan[181], C. Gubbels[175], J. Guenther[36], A. Guerguichon[65], J.G.R. Guerrero Rojas[174], F. Guescini[115], D. Guest[171], R. Gugel[52], T. Guillemin[5], S. Guindon[36], U. Gul[57], J. Guo[60c], W. Guo[106], Y. Guo[60a], Z. Guo[102], R. Gupta[46], S. Gurbuz[12c], G. Gustavino[129], M. Guth[52], P. Gutierrez[129], C. Gutschow[95], C. Guyot[145], C. Gwenlan[135], C.B. Gwilliam[91], A. Haas[125], C. Haber[18], H.K. Hadavand[8], A. Hadef[60a], M. Haleem[177], J. Haley[130], G. Halladjian[107], G.D. Hallewell[102], K. Hamacher[182], P. Hamal[131], K. Hamano[176], H. Hamdaoui[35e], M. Hamer[24], G.N. Hamity[50], K. Han[60a,x], L. Han[60a], S. Han[15a], Y.F. Han[167], K. Hanagaki[82,v], M. Hance[146], D.M. Handl[114], B. Haney[137], R. Hankache[136], E. Hansen[97], J.B. Hansen[40], J.D. Hansen[40], M.C. Hansen[24], P.H. Hansen[40], E.C. Hanson[101], K. Hara[169], T. Harenberg[182], S. Harkusha[108], P.F. Harrison[178], N.M. Hartmann[114], Y. Hasegawa[150], A. Hasib[50], S. Hassani[145], S. Haug[20], R. Hauser[107], L.B. Havener[39], M. Havranek[142], C.M. Hawkes[21], R.J. Hawkings[36], D. Hayden[107], C. Hayes[106], R.L. Hayes[175], C.P. Hays[135], J.M. Hays[93], H.S. Hayward[91], S.J. Haywood[144], F. He[60a], M.P. Heath[50], V. Hedberg[97], S. Heer[24], K.K. Heidegger[52], W.D. Heidorn[79], J. Heilman[34], S. Heim[46], T. Heim[18], B. Heinemann[46,an], J.J. Heinrich[132], L. Heinrich[36], J. Hejbal[141], L. Helary[61b], A. Held[125], S. Hellesund[134], C.M. Helling[146], S. Hellman[45a,45b], C. Helsens[36], R.C.W. Henderson[90], Y. Heng[181], L. Henkelmann[61a], S. Henkelmann[175], A.M. Henriques Correia[36], H. Herde[26], V. Herget[177], Y. Hernández Jiménez[33e], H. Herr[100], M.G. Herrmann[114], T. Herrmann[48], G. Herten[52], R. Hertenberger[114], L. Hervas[36], T.C. Herwig[137], G.G. Hesketh[95], N.P. Hessey[168a],

JHEP07(2020)124

A. Higashida[163], S. Higashino[82], E. Higón-Rodriguez[174], K. Hildebrand[37], J.C. Hill[32], K.K. Hill[29], K.H. Hiller[46], S.J. Hillier[21], M. Hils[48], I. Hinchliffe[18], F. Hinterkeuser[24], M. Hirose[133], S. Hirose[52], D. Hirschbuehl[182], B. Hiti[92], O. Hladik[141], D.R. Hlaluku[33e], X. Hoad[50], J. Hobbs[155], N. Hod[180], M.C. Hodgkinson[149], A. Hoecker[36], D. Hohn[52], D. Hohov[65], T. Holm[24], T.R. Holmes[37], M. Holzbock[114], L.B.A.H. Hommels[32], S. Honda[169], T.M. Hong[139], J.C. Honig[52], A. Hönle[115], B.H. Hooberman[173], W.H. Hopkins[6], Y. Horii[117], P. Horn[48], L.A. Horyn[37], S. Hou[158], A. Hoummada[35a], J. Howarth[101], J. Hoya[89], M. Hrabovsky[131], J. Hrdinka[77], I. Hristova[19], J. Hrivnac[65], A. Hrynevich[109], T. Hryn'ova[5], P.J. Hsu[64], S.-C. Hsu[148], Q. Hu[29], S. Hu[60c], Y.F. Hu[15a,15d], D.P. Huang[95], Y. Huang[60a], Y. Huang[15a], Z. Hubacek[142], F. Hubaut[102], M. Huebner[24], F. Huegging[24], T.B. Huffman[135], M. Huhtinen[36], R.F.H. Hunter[34], P. Huo[155], N. Huseynov[80,ae], J. Huston[107], J. Huth[59], R. Hyneman[106], S. Hyrych[28a], G. Iacobucci[54], G. Iakovidis[29], I. Ibragimov[151], L. Iconomidou-Fayard[65], P. Iengo[36], R. Ignazzi[40], O. Igonkina[120,aa,*], R. Iguchi[163], T. Iizawa[54], Y. Ikegami[82], M. Ikeno[82], D. Iliadis[162], N. Ilic[119,167,ad], F. Iltzsche[48], G. Introzzi[71a,71b], M. Iodice[75a], K. Iordanidou[168a], V. Ippolito[73a,73b], M.F. Isacson[172], M. Ishino[163], W. Islam[130], C. Issever[19,46], S. Istin[160], F. Ito[169], J.M. Iturbe Ponce[63a], R. Iuppa[76a,76b], A. Ivina[180], H. Iwasaki[82], J.M. Izen[43], V. Izzo[70a], P. Jacka[141], P. Jackson[1], R.M. Jacobs[24], B.P. Jaeger[152], V. Jain[2], G. Jäkel[182], K.B. Jakobi[100], K. Jakobs[52], T. Jakoubek[141], J. Jamieson[57], K.W. Janas[84a], R. Jansky[54], M. Janus[53], P.A. Janus[84a], G. Jarlskog[97], N. Javadov[80,ae], T. Javůrek[36], M. Javurkova[103], F. Jeanneau[145], L. Jeanty[132], J. Jejelava[159a], A. Jelinskas[178], P. Jenni[52,b], N. Jeong[46], S. Jézéquel[5], H. Ji[181], J. Jia[155], H. Jiang[79], Y. Jiang[60a], Z. Jiang[153,p], S. Jiggins[52], F.A. Jimenez Morales[38], J. Jimenez Pena[115], S. Jin[15c], A. Jinaru[27b], O. Jinnouchi[165], H. Jivan[33e], P. Johansson[149], K.A. Johns[7], C.A. Johnson[66], R.W.L. Jones[90], S.D. Jones[156], S. Jones[7], T.J. Jones[91], J. Jongmanns[61a], P.M. Jorge[140a], J. Jovicevic[36], X. Ju[18], J.J. Junggeburth[115], A. Juste Rozas[14,y], A. Kaczmarska[85], M. Kado[73a,73b], H. Kagan[127], M. Kagan[153], A. Kahn[39], C. Kahra[100], T. Kaji[179], E. Kajomovitz[160], C.W. Kalderon[29], A. Kaluza[100], A. Kamenshchikov[123], M. Kaneda[163], N.J. Kang[146], S. Kang[79], L. Kanjir[92], Y. Kano[117], V.A. Kantserov[112], J. Kanzaki[82], L.S. Kaplan[181], D. Kar[33e], K. Karava[135], M.J. Kareem[168b], S.N. Karpov[80], Z.M. Karpova[80], V. Kartvelishvili[90], A.N. Karyukhin[123], L. Kashif[181], A. Kastanas[45a,45b], C. Kato[60d,60c], J. Katzy[46], K. Kawade[150], K. Kawagoe[88], T. Kawaguchi[117], T. Kawamoto[145], G. Kawamura[53], E.F. Kay[176], V.F. Kazanin[122b,122a], R. Keeler[176], R. Kehoe[42], J.S. Keller[34], E. Kellermann[97], D. Kelsey[156], J.J. Kempster[21], J. Kendrick[21], K.E. Kennedy[39], O. Kepka[141], S. Kersten[182], B.P. Kerševan[92], S. Ketabchi Haghighat[167], M. Khader[173], F. Khalil-Zada[13], M. Khandoga[145], A. Khanov[130], A.G. Kharlamov[122b,122a], T. Kharlamova[122b,122a], E.E. Khoda[175], A. Khodinov[166], T.J. Khoo[54], E. Khramov[80], J. Khubua[159b], S. Kido[83], M. Kiehn[54], C.R. Kilby[94], E. Kim[165], Y.K. Kim[37], N. Kimura[95], O.M. Kind[19], B.T. King[91,*], D. Kirchmeier[48], J. Kirk[144], A.E. Kiryunin[115], T. Kishimoto[163], D.P. Kisliuk[167], V. Kitali[46], O. Kivernyk[5], T. Klapdor-Kleingrothaus[52], M. Klassen[61a], C. Klein[32], M.H. Klein[106], M. Klein[91], U. Klein[91], K. Kleinknecht[100], P. Klimek[121], A. Klimentov[29], T. Klingl[24], T. Klioutchnikova[36], F.F. Klitzner[114], P. Kluit[120], S. Kluth[115], E. Kneringer[77], E.B.F.G. Knoops[102], A. Knue[52], D. Kobayashi[88], T. Kobayashi[163], M. Kobel[48], M. Kocian[153], T. Kodama[163], P. Kodys[143], P.T. Koenig[24], T. Koffas[34], N.M. Köhler[36], M. Kolb[145], I. Koletsou[5], T. Komarek[131], T. Kondo[82], K. Köneke[52], A.X.Y. Kong[1], A.C. König[119], T. Kono[126], R. Konoplich[125,ai], V. Konstantinides[95], N. Konstantinidis[95], B. Konya[97], R. Kopeliansky[66], S. Koperny[84a], K. Korcyl[85], K. Kordas[162], G. Koren[161], A. Korn[95], I. Korolkov[14], E.V. Korolkova[149], N. Korotkova[113], O. Kortner[115], S. Kortner[115], T. Kosek[143], V.V. Kostyukhin[149,166], A. Kotsokechagia[65], A. Kotwal[49], A. Koulouris[10], A. Kourkoumeli-Charalampidi[71a,71b], C. Kourkoumelis[9], E. Kourlitis[149], V. Kouskoura[29], A.B. Kowalewska[85], R. Kowalewski[176], W. Kozanecki[101], A.S. Kozhin[123],

JHEP07(2020)124

V.A. Kramarenko[113], G. Kramberger[92], D. Krasnopevtsev[60a], M.W. Krasny[136], A. Krasznahorkay[36], D. Krauss[115], J.A. Kremer[84a], J. Kretzschmar[91], P. Krieger[167], F. Krieter[114], A. Krishnan[61b], K. Krizka[18], K. Kroeninger[47], H. Kroha[115], J. Kroll[141], J. Kroll[137], K.S. Krowpman[107], U. Kruchonak[80], H. Krüger[24], N. Krumnack[79], M.C. Kruse[49], J.A. Krzysiak[85], T. Kubota[105], O. Kuchinskaia[166], S. Kuday[4b], J.T. Kuechler[46], S. Kuehn[36], A. Kugel[61a], T. Kuhl[46], V. Kukhtin[80], R. Kukla[102], Y. Kulchitsky[108,ag], S. Kuleshov[147d], Y.P. Kulinich[173], M. Kuna[58], T. Kunigo[86], A. Kupco[141], T. Kupfer[47], O. Kuprash[52], H. Kurashige[83], L.L. Kurchaninov[168a], Y.A. Kurochkin[108], A. Kurova[112], M.G. Kurth[15a,15d], E.S. Kuwertz[36], M. Kuze[165], A.K. Kvam[148], J. Kvita[131], T. Kwan[104], L. La Rotonda[41b,41a], F. La Ruffa[41b,41a], C. Lacasta[174], F. Lacava[73a,73b], D.P.J. Lack[101], H. Lacker[19], D. Lacour[136], E. Ladygin[80], R. Lafaye[5], B. Laforge[136], T. Lagouri[147b], S. Lai[53], I.K. Lakomiec[84a], S. Lammers[66], W. Lampl[7], C. Lampoudis[162], E. Lançon[29], U. Landgraf[52], M.P.J. Landon[93], M.C. Lanfermann[54], V.S. Lang[46], J.C. Lange[53], R.J. Langenberg[103], A.J. Lankford[171], F. Lanni[29], K. Lantzsch[24], A. Lanza[71a], A. Lapertosa[55b,55a], S. Laplace[136], J.F. Laporte[145], T. Lari[69a], F. Lasagni Manghi[23b,23a], M. Lassnig[36], T.S. Lau[63a], A. Laudrain[65], A. Laurier[34], M. Lavorgna[70a,70b], S.D. Lawlor[94], M. Lazzaroni[69a,69b], B. Le[105], E. Le Guirriec[102], A. Lebedev[79], M. LeBlanc[7], T. LeCompte[6], F. Ledroit-Guillon[58], A.C.A. Lee[95], C.A. Lee[29], G.R. Lee[17], L. Lee[59], S.C. Lee[158], S. Lee[79], B. Lefebvre[168a], H.P. Lefebvre[94], M. Lefebvre[176], C. Leggett[18], K. Lehmann[152], N. Lehmann[182], G. Lehmann Miotto[36], W.A. Leight[46], A. Leisos[162,w], M.A.L. Leite[81d], C.E. Leitgeb[114], R. Leitner[143], D. Lellouch[180,*], K.J.C. Leney[42], T. Lenz[24], R. Leone[7], S. Leone[72a], C. Leonidopoulos[50], A. Leopold[136], C. Leroy[110], R. Les[167], C.G. Lester[32], M. Levchenko[138], J. Levêque[5], D. Levin[106], L.J. Levinson[180], D.J. Lewis[21], B. Li[15b], B. Li[106], C-Q. Li[60a], F. Li[60c], H. Li[60a], H. Li[60b], J. Li[60c], K. Li[148], L. Li[60c], M. Li[15a,15d], Q. Li[15a,15d], Q.Y. Li[60a], S. Li[60d,60c], X. Li[46], Y. Li[46], Z. Li[60b], Z. Li[104], Z. Liang[15a], B. Liberti[74a], A. Liblong[167], K. Lie[63c], S. Lim[29], C.Y. Lin[32], K. Lin[107], T.H. Lin[100], R.A. Linck[66], J.H. Lindon[21], A.L. Lionti[54], E. Lipeles[137], A. Lipniacka[17], T.M. Liss[173,ao], A. Lister[175], J.D. Little[8], B. Liu[79], B.L. Liu[6], H.B. Liu[29], H. Liu[106], J.B. Liu[60a], J.K.K. Liu[37], K. Liu[60d], M. Liu[60a], P. Liu[15a], Y. Liu[46], Y. Liu[15a,15d], Y.L. Liu[106], Y.W. Liu[60a], M. Livan[71a,71b], A. Lleres[58], J. Llorente Merino[152], S.L. Lloyd[93], C.Y. Lo[63b], E.M. Lobodzinska[46], P. Loch[7], S. Loffredo[74a,74b], T. Lohse[19], K. Lohwasser[149], M. Lokajicek[141], J.D. Long[173], R.E. Long[90], L. Longo[36], K.A. Looper[127], J.A. Lopez[147d], I. Lopez Paz[101], A. Lopez Solis[149], J. Lorenz[114], N. Lorenzo Martinez[5], A.M. Lory[114], M. Losada[22a], P.J. Lösel[114], A. Lösle[52], X. Lou[46], X. Lou[15a], A. Lounis[65], J. Love[6], P.A. Love[90], J.J. Lozano Bahilo[174], M. Lu[60a], Y.J. Lu[64], H.J. Lubatti[148], C. Luci[73a,73b], A. Lucotte[58], C. Luedtke[52], F. Luehring[66], I. Luise[136], L. Luminari[73a], B. Lund-Jensen[154], M.S. Lutz[103], D. Lynn[29], H. Lyons[91], R. Lysak[141], E. Lytken[97], F. Lyu[15a], V. Lyubushkin[80], T. Lyubushkina[80], H. Ma[29], L.L. Ma[60b], Y. Ma[60b], G. Maccarrone[51], A. Macchiolo[115], C.M. Macdonald[149], J. Machado Miguens[137], D. Madaffari[174], R. Madar[38], W.F. Mader[48], M. Madugoda Ralalage Don[130], N. Madysa[48], J. Maeda[83], T. Maeno[29], M. Maerker[48], V. Magerl[52], N. Magini[79], D.J. Mahon[39], C. Maidantchik[81b], T. Maier[114], A. Maio[140a,140b,140d], K. Maj[84a], O. Majersky[28a], S. Majewski[132], Y. Makida[82], N. Makovec[65], B. Malaescu[136], Pa. Malecki[85], V.P. Maleev[138], F. Malek[58], U. Mallik[78], D. Malon[6], C. Malone[32], S. Maltezos[10], S. Malyukov[80], J. Mamuzic[174], G. Mancini[51], I. Mandić[92], L. Manhaes de Andrade Filho[81a], I.M. Maniatis[162], J. Manjarres Ramos[48], K.H. Mankinen[97], A. Mann[114], A. Manousos[77], B. Mansoulie[145], I. Manthos[162], S. Manzoni[120], A. Marantis[162], G. Marceca[30], L. Marchese[135], G. Marchiori[136], M. Marcisovsky[141], L. Marcoccia[74a,74b], C. Marcon[97], C.A. Marin Tobon[36], M. Marjanovic[129], Z. Marshall[18], M.U.F. Martensson[172], S. Marti-Garcia[174], C.B. Martin[127], T.A. Martin[178], V.J. Martin[50], B. Martin dit Latour[17], L. Martinelli[75a,75b], M. Martinez[14,y], V.I. Martinez Outschoorn[103], S. Martin-Haugh[144],

JHEP07(2020)124

V.S. Martoiu[27b], A.C. Martyniuk[95], A. Marzin[36], S.R. Maschek[115], L. Masetti[100], T. Mashimo[163], R. Mashinistov[111], J. Masik[101], A.L. Maslennikov[122b,122a], L. Massa[23b,23a], P. Massarotti[70a,70b], P. Mastrandrea[72a,72b], A. Mastroberardino[41b,41a], T. Masubuchi[163], D. Matakias[29], A. Matic[114], N. Matsuzawa[163], P. Mättig[24], J. Maurer[27b], B. Maček[92], D.A. Maximov[122b,122a], R. Mazini[158], I. Maznas[162], S.M. Mazza[146], S.P. Mc Kee[106], T.G. McCarthy[115], W.P. McCormack[18], E.F. McDonald[105], J.A. Mcfayden[36], G. Mchedlidze[159b], M.A. McKay[42], K.D. McLean[176], S.J. McMahon[144], P.C. McNamara[105], C.J. McNicol[178], R.A. McPherson[176,ad], J.E. Mdhluli[33e], Z.A. Meadows[103], S. Meehan[36], T. Megy[52], S. Mehlhase[114], A. Mehta[91], T. Meideck[58], B. Meirose[43], D. Melini[160], B.R. Mellado Garcia[33e], J.D. Mellenthin[53], M. Melo[28a], F. Meloni[46], A. Melzer[24], S.B. Menary[101], E.D. Mendes Gouveia[140a,140e], L. Meng[36], X.T. Meng[106], S. Menke[115], E. Meoni[41b,41a], S. Mergelmeyer[19], S.A.M. Merkt[139], C. Merlassino[135], P. Mermod[54], L. Merola[70a,70b], C. Meroni[69a], G. Merz[106], O. Meshkov[113,111], J.K.R. Meshreki[151], A. Messina[73a,73b], J. Metcalfe[6], A.S. Mete[6], C. Meyer[66], J-P. Meyer[145], H. Meyer Zu Theenhausen[61a], F. Miano[156], M. Michetti[19], R.P. Middleton[144], L. Mijović[50], G. Mikenberg[180], M. Mikestikova[141], M. Mikuž[92], H. Mildner[149], M. Milesi[105], A. Milic[167], D.A. Millar[93], D.W. Miller[37], A. Milov[180], D.A. Milstead[45a,45b], R.A. Mina[153], A.A. Minaenko[123], M. Miñano Moya[174], I.A. Minashvili[159b], A.I. Mincer[125], B. Mindur[84a], M. Mineev[80], Y. Minegishi[163], L.M. Mir[14], A. Mirto[68a,68b], K.P. Mistry[137], T. Mitani[179], J. Mitrevski[114], V.A. Mitsou[174], M. Mittal[60c], O. Miu[167], A. Miucci[20], P.S. Miyagawa[149], A. Mizukami[82], J.U. Mjörnmark[97], T. Mkrtchyan[61a], M. Mlynarikova[143], T. Moa[45a,45b], K. Mochizuki[110], P. Mogg[52], S. Mohapatra[39], R. Moles-Valls[24], M.C. Mondragon[107], K. Mönig[46], J. Monk[40], E. Monnier[102], A. Montalbano[152], J. Montejo Berlingen[36], M. Montella[95], F. Monticelli[89], S. Monzani[69a], N. Morange[65], D. Moreno[22a], M. Moreno Llácer[174], C. Moreno Martinez[14], P. Morettini[55b], M. Morgenstern[160], S. Morgenstern[48], D. Mori[152], M. Morii[59], M. Morinaga[179], V. Morisbak[134], A.K. Morley[36], G. Mornacchi[36], A.P. Morris[95], L. Morvaj[155], P. Moschovakos[36], B. Moser[120], M. Mosidze[159b], T. Moskalets[145], H.J. Moss[149], J. Moss[31,m], E.J.W. Moyse[103], S. Muanza[102], J. Mueller[139], R.S.P. Mueller[114], D. Muenstermann[90], G.A. Mullier[97], D.P. Mungo[69a,69b], J.L. Munoz Martinez[14], F.J. Munoz Sanchez[101], P. Murin[28b], W.J. Murray[178,144], A. Murrone[69a,69b], M. Muškinja[18], C. Mwewa[33a], A.G. Myagkov[123,aj], A.A. Myers[139], J. Myers[132], M. Myska[142], B.P. Nachman[18], O. Nackenhorst[47], A.Nag Nag[48], K. Nagai[135], K. Nagano[82], Y. Nagasaka[62], J.L. Nagle[29], E. Nagy[102], A.M. Nairz[36], Y. Nakahama[117], K. Nakamura[82], T. Nakamura[163], I. Nakano[128], H. Nanjo[133], F. Napolitano[61a], R.F. Naranjo Garcia[46], R. Narayan[42], I. Naryshkin[138], T. Naumann[46], G. Navarro[22a], P.Y. Nechaeva[111], F. Nechansky[46], T.J. Neep[21], A. Negri[71a,71b], M. Negrini[23b], C. Nellist[119], M.E. Nelson[45a,45b], S. Nemecek[141], M. Nessi[36,d], M.S. Neubauer[173], F. Neuhaus[100], M. Neumann[182], R. Newhouse[175], P.R. Newman[21], C.W. Ng[139], Y.S. Ng[19], Y.W.Y. Ng[171], B. Ngair[35e], H.D.N. Nguyen[102], T. Nguyen Manh[110], E. Nibigira[38], R.B. Nickerson[135], R. Nicolaidou[145], D.S. Nielsen[40], J. Nielsen[146], N. Nikiforou[11], V. Nikolaenko[123,aj], I. Nikolic-Audit[136], K. Nikolopoulos[21], P. Nilsson[29], H.R. Nindhito[54], Y. Ninomiya[82], A. Nisati[73a], N. Nishu[60c], R. Nisius[115], I. Nitsche[47], T. Nitta[179], T. Nobe[163], Y. Noguchi[86], I. Nomidis[136], M.A. Nomura[29], M. Nordberg[36], T. Novak[92], O. Novgorodova[48], R. Novotny[142], L. Nozka[131], K. Ntekas[171], E. Nurse[95], F.G. Oakham[34,ap], H. Oberlack[115], J. Ocariz[136], A. Ochi[83], I. Ochoa[39], J.P. Ochoa-Ricoux[147a], K. O'Connor[26], S. Oda[88], S. Odaka[82], S. Oerdek[53], A. Ogrodnik[84a], A. Oh[101], S.H. Oh[49], C.C. Ohm[154], H. Oide[165], M.L. Ojeda[167], H. Okawa[169], Y. Okazaki[86], M.W. O'Keefe[91], Y. Okumura[163], T. Okuyama[82], A. Olariu[27b], L.F. Oleiro Seabra[140a], S.A. Olivares Pino[147a], D. Oliveira Damazio[29], J.L. Oliver[1], M.J.R. Olsson[171], A. Olszewski[85], J. Olszowska[85], D.C. O'Neil[152], A.P. O'neill[135], A. Onofre[140a,140e], P.U.E. Onyisi[11], H. Oppen[134], M.J. Oreglia[37], G.E. Orellana[89], D. Orestano[75a,75b], N. Orlando[14], R.S. Orr[167], V. O'Shea[57],

JHEP07(2020)124

R. Ospanov[60a], G. Otero y Garzon[30], H. Otono[88], P.S. Ott[61a], M. Ouchrif[35d], J. Ouellette[29], F. Ould-Saada[134], A. Ouraou[145], Q. Ouyang[15a], M. Owen[57], R.E. Owen[21], V.E. Ozcan[12c], N. Ozturk[8], J. Pacalt[131], H.A. Pacey[32], K. Pachal[49], A. Pacheco Pages[14], C. Padilla Aranda[14], S. Pagan Griso[18], M. Paganini[183], G. Palacino[66], S. Palazzo[50], S. Palestini[36], M. Palka[84b], D. Pallin[38], P. Palni[84a], I. Panagoulias[10], C.E. Pandini[36], J.G. Panduro Vazquez[94], P. Pani[46], G. Panizzo[67a,67c], L. Paolozzi[54], C. Papadatos[110], K. Papageorgiou[9,g], S. Parajuli[42], A. Paramonov[6], D. Paredes Hernandez[63b], S.R. Paredes Saenz[135], B. Parida[166], T.H. Park[167], A.J. Parker[31], M.A. Parker[32], F. Parodi[55b,55a], E.W. Parrish[121], J.A. Parsons[39], U. Parzefall[52], L. Pascual Dominguez[136], V.R. Pascuzzi[167], J.M.P. Pasner[146], F. Pasquali[120], E. Pasqualucci[73a], S. Passaggio[55b], F. Pastore[94], P. Pasuwan[45a,45b], S. Pataraia[100], J.R. Pater[101], A. Pathak[181,i], J. Patton[91], T. Pauly[36], J. Pearkes[153], B. Pearson[115], M. Pedersen[134], L. Pedraza Diaz[119], R. Pedro[140a], T. Peiffer[53], S.V. Peleganchuk[122b,122a], O. Penc[141], H. Peng[60a], B.S. Peralva[81a], M.M. Perego[65], A.P. Pereira Peixoto[140a], D.V. Perepelitsa[29], F. Peri[19], L. Perini[69a,69b], H. Pernegger[36], S. Perrella[140a], A. Perrevoort[120], K. Peters[46], R.F.Y. Peters[101], B.A. Petersen[36], T.C. Petersen[40], E. Petit[102], A. Petridis[1], C. Petridou[162], P. Petroff[65], M. Petrov[135], F. Petrucci[75a,75b], M. Pettee[183], N.E. Pettersson[103], K. Petukhova[143], A. Peyaud[145], R. Pezoa[147d], L. Pezzotti[71a,71b], T. Pham[105], F.H. Phillips[107], P.W. Phillips[144], M.W. Phipps[173], G. Piacquadio[155], E. Pianori[18], A. Picazio[103], R.H. Pickles[101], R. Piegaia[30], D. Pietreanu[27b], J.E. Pilcher[37], A.D. Pilkington[101], M. Pinamonti[67a,67c], J.L. Pinfold[3], M. Pitt[161], L. Pizzimento[74a,74b], M.-A. Pleier[29], V. Pleskot[143], E. Plotnikova[80], P. Podberezko[122b,122a], R. Poettgen[97], R. Poggi[54], L. Poggioli[136], I. Pogrebnyak[107], D. Pohl[24], I. Pokharel[53], G. Polesello[71a], A. Poley[18], A. Policicchio[73a,73b], R. Polifka[143], A. Polini[23b], C.S. Pollard[46], V. Polychronakos[29], D. Ponomarenko[112], L. Pontecorvo[36], S. Popa[27a], G.A. Popeneciu[27d], L. Portales[5], D.M. Portillo Quintero[58], S. Pospisil[142], K. Potamianos[46], I.N. Potrap[80], C.J. Potter[32], H. Potti[11], T. Poulsen[97], J. Poveda[36], T.D. Powell[149], G. Pownall[46], M.E. Pozo Astigarraga[36], P. Pralavorio[102], S. Prell[79], D. Price[101], M. Primavera[68a], S. Prince[104], M.L. Proffitt[148], N. Proklova[112], K. Prokofiev[63c], F. Prokoshin[80], S. Protopopescu[29], J. Proudfoot[6], M. Przybycien[84a], D. Pudzha[138], A. Puri[173], P. Puzo[65], J. Qian[106], Y. Qin[101], A. Quadt[53], M. Queitsch-Maitland[36], A. Qureshi[1], M. Racko[28a], F. Ragusa[69a,69b], G. Rahal[98], J.A. Raine[54], S. Rajagopalan[29], A. Ramirez Morales[93], K. Ran[15a,15d], T. Rashid[65], S. Raspopov[5], D.M. Rauch[46], F. Rauscher[114], S. Rave[100], B. Ravina[149], I. Ravinovich[180], J.H. Rawling[101], M. Raymond[36], A.L. Read[134], N.P. Readioff[58], M. Reale[68a,68b], D.M. Rebuzzi[71a,71b], A. Redelbach[177], G. Redlinger[29], K. Reeves[43], L. Rehnisch[19], J. Reichert[137], D. Reikher[161], A. Reiss[100], A. Rej[151], C. Rembser[36], A. Renardi[46], M. Renda[27b], M. Rescigno[73a], S. Resconi[69a], E.D. Resseguie[18], S. Rettie[95], B. Reynolds[127], E. Reynolds[21], O.L. Rezanova[122b,122a], P. Reznicek[143], E. Ricci[76a,76b], R. Richter[115], S. Richter[46], E. Richter-Was[84b], O. Ricken[24], M. Ridel[136], P. Rieck[115], O. Rifki[46], M. Rijssenbeek[155], A. Rimoldi[71a,71b], M. Rimoldi[46], L. Rinaldi[23b], G. Ripellino[154], I. Riu[14], J.C. Rivera Vergara[176], F. Rizatdinova[130], E. Rizvi[93], C. Rizzi[36], R.T. Roberts[101], S.H. Robertson[104,ad], M. Robin[46], D. Robinson[32], C.M. Robles Gajardo[147d], M. Robles Manzano[100], A. Robson[57], A. Rocchi[74a,74b], E. Rocco[100], C. Roda[72a,72b], S. Rodriguez Bosca[174], A. Rodriguez Perez[14], D. Rodriguez Rodriguez[174], A.M. Rodríguez Vera[168b], S. Roe[36], O. Røhne[134], R. Röhrig[115], R.A. Rojas[147d], B. Roland[52], C.P.A. Roland[66], J. Roloff[29], A. Romaniouk[112], M. Romano[23b,23a], N. Rompotis[91], M. Ronzani[125], L. Roos[136], S. Rosati[73a], G. Rosin[103], B.J. Rosser[137], E. Rossi[46], E. Rossi[75a,75b], E. Rossi[70a,70b], L.P. Rossi[55b], L. Rossini[69a,69b], R. Rosten[14], M. Rotaru[27b], J. Rothberg[148], B. Rottler[52], D. Rousseau[65], G. Rovelli[71a,71b], A. Roy[11], D. Roy[33e], A. Rozanov[102], Y. Rozen[160], X. Ruan[33e], F. Rühr[52], A. Ruiz-Martinez[174], A. Rummler[36], Z. Rurikova[52], N.A. Rusakovich[80], H.L. Russell[104], L. Rustige[38,47], J.P. Rutherfoord[7], E.M. Rüttinger[149], M. Rybar[39], G. Rybkin[65],

JHEP07(2020)124

E.B. Rye[134], A. Ryzhov[123], J.A. Sabater Iglesias[46], P. Sabatini[53], G. Sabato[120], S. Sacerdoti[65], H.F-W. Sadrozinski[146], R. Sadykov[80], F. Safai Tehrani[73a], B. Safarzadeh Samani[156], M. Safdari[153], P. Saha[121], S. Saha[104], M. Sahinsoy[61a], A. Sahu[182], M. Saimpert[46], M. Saito[163], T. Saito[163], H. Sakamoto[163], A. Sakharov[125,ai], D. Salamani[54], G. Salamanna[75a,75b], J.E. Salazar Loyola[147d], A. Salnikov[153], J. Salt[174], D. Salvatore[41b,41a], F. Salvatore[156], A. Salvucci[63a,63b,63c], A. Salzburger[36], J. Samarati[36], D. Sammel[52], D. Sampsonidis[162], D. Sampsonidou[162], J. Sánchez[174], A. Sanchez Pineda[67a,36,67c], H. Sandaker[134], C.O. Sander[46], I.G. Sanderswood[90], M. Sandhoff[182], C. Sandoval[22a], D.P.C. Sankey[144], M. Sannino[55b,55a], Y. Sano[117], A. Sansoni[51], C. Santoni[38], H. Santos[140a,140b], S.N. Santpur[18], A. Santra[174], A. Sapronov[80], J.G. Saraiva[140a,140d], O. Sasaki[82], K. Sato[169], F. Sauerburger[52], E. Sauvan[5], P. Savard[167,ap], R. Sawada[163], C. Sawyer[144], L. Sawyer[96,ah], C. Sbarra[23b], A. Sbrizzi[23a], T. Scanlon[95], J. Schaarschmidt[148], P. Schacht[115], B.M. Schachtner[114], D. Schaefer[37], L. Schaefer[137], J. Schaeffer[100], S. Schaepe[36], U. Schäfer[100], A.C. Schaffer[65], D. Schaile[114], R.D. Schamberger[155], N. Scharmberg[101], V.A. Schegelsky[138], D. Scheirich[143], F. Schenck[19], M. Schernau[171], C. Schiavi[55b,55a], L.K. Schildgen[24], Z.M. Schillaci[26], E.J. Schioppa[36], M. Schioppa[41b,41a], K.E. Schleicher[52], S. Schlenker[36], K.R. Schmidt-Sommerfeld[115], K. Schmieden[36], C. Schmitt[100], S. Schmitt[46], S. Schmitz[100], J.C. Schmoeckel[46], L. Schoeffel[145], A. Schoening[61b], P.G. Scholer[52], E. Schopf[135], M. Schott[100], J.F.P. Schouwenberg[119], J. Schovancova[36], S. Schramm[54], F. Schroeder[182], A. Schulte[100], H-C. Schultz-Coulon[61a], M. Schumacher[52], B.A. Schumm[146], Ph. Schune[145], A. Schwartzman[153], T.A. Schwarz[106], Ph. Schwemling[145], R. Schwienhorst[107], A. Sciandra[146], G. Sciolla[26], M. Scodeggio[46], M. Scornajenghi[41b,41a], F. Scuri[72a], F. Scutti[105], L.M. Scyboz[115], C.D. Sebastiani[73a,73b], P. Seema[19], S.C. Seidel[118], A. Seiden[146], B.D. Seidlitz[29], T. Seiss[37], J.M. Seixas[81b], G. Sekhniaidze[70a], S.J. Sekula[42], N. Semprini-Cesari[23b,23a], S. Sen[49], C. Serfon[77], L. Serin[65], L. Serkin[67a,67b], M. Sessa[60a], H. Severini[129], S. Sevova[153], T. Šfiligoj[92], F. Sforza[55b,55a], A. Sfyrla[54], E. Shabalina[53], J.D. Shahinian[146], N.W. Shaikh[45a,45b], D. Shaked Renous[180], L.Y. Shan[15a], J.T. Shank[25], M. Shapiro[18], A. Sharma[135], A.S. Sharma[1], P.B. Shatalov[124], K. Shaw[156], S.M. Shaw[101], M. Shehade[180], Y. Shen[129], A.D. Sherman[25], P. Sherwood[95], L. Shi[158], S. Shimizu[82], C.O. Shimmin[183], Y. Shimogama[179], M. Shimojima[116], I.P.J. Shipsey[135], S. Shirabe[165], M. Shiyakova[80,ab], J. Shlomi[180], A. Shmeleva[111], M.J. Shochet[37], J. Shojaii[105], D.R. Shope[129], S. Shrestha[127], E.M. Shrif[33e], E. Shulga[180], P. Sicho[141], A.M. Sickles[173], P.E. Sidebo[154], E. Sideras Haddad[33e], O. Sidiropoulou[36], A. Sidoti[23b,23a], F. Siegert[48], Dj. Sijacki[16], M.Jr. Silva[181], M.V. Silva Oliveira[81a], S.B. Silverstein[45a], S. Simion[65], R. Simoniello[100], S. Simsek[12b], P. Sinervo[167], V. Sinetckii[113], N.B. Sinev[132], S. Singh[152], M. Sioli[23b,23a], I. Siral[132], S.Yu. Sivoklokov[113], J. Sjölin[45a,45b], E. Skorda[97], P. Skubic[129], M. Slawinska[85], K. Sliwa[170], R. Slovak[143], V. Smakhtin[180], B.H. Smart[144], J. Smiesko[28b], N. Smirnov[112], S.Yu. Smirnov[112], Y. Smirnov[112], L.N. Smirnova[113,t], O. Smirnova[97], J.W. Smith[53], M. Smizanska[90], K. Smolek[142], A. Smykiewicz[85], A.A. Snesarev[111], H.L. Snoek[120], I.M. Snyder[132], S. Snyder[29], R. Sobie[176,ad], A. Soffer[161], A. Søgaard[50], F. Sohns[53], C.A. Solans Sanchez[36], E.Yu. Soldatov[112], U. Soldevila[174], A.A. Solodkov[123], A. Soloshenko[80], O.V. Solovyanov[123], V. Solovyev[138], P. Sommer[149], H. Son[170], W. Song[144], W.Y. Song[168b], A. Sopczak[142], A.L. Sopio[95], F. Sopkova[28b], C.L. Sotiropoulou[72a,72b], S. Sottocornola[71a,71b], R. Soualah[67a,67c,f], A.M. Soukharev[122b,122a], D. South[46], S. Spagnolo[68a,68b], M. Spalla[115], M. Spangenberg[178], F. Spanò[94], D. Sperlich[52], T.M. Spieker[61a], G. Spigo[36], M. Spina[156], D.P. Spiteri[57], M. Spousta[143], A. Stabile[69a,69b], B.L. Stamas[121], R. Stamen[61a], M. Stamenkovic[120], E. Stanecka[85], B. Stanislaus[135], M.M. Stanitzki[46], M. Stankaityte[135], B. Stapf[120], E.A. Starchenko[123], G.H. Stark[146], J. Stark[58], P. Staroba[141], P. Starovoitov[61a], S. Stärz[104], R. Staszewski[85], G. Stavropoulos[44], M. Stegler[46], P. Steinberg[29], A.L. Steinhebel[132],

JHEP07(2020)124

B. Stelzer[152], H.J. Stelzer[139], O. Stelzer-Chilton[168a], H. Stenzel[56], T.J. Stevenson[156], G.A. Stewart[36], M.C. Stockton[36], G. Stoicea[27b], M. Stolarski[140a], S. Stonjek[115], A. Straessner[48], J. Strandberg[154], S. Strandberg[45a,45b], M. Strauss[129], P. Strizenec[28b], R. Ströhmer[177], D.M. Strom[132], R. Stroynowski[42], A. Strubig[50], S.A. Stucci[29], B. Stugu[17], J. Stupak[129], N.A. Styles[46], D. Su[153], W. Su[60c], S. Suchek[61a], V.V. Sulin[111], M.J. Sullivan[91], D.M.S. Sultan[54], S. Sultansoy[4c], T. Sumida[86], S. Sun[106], X. Sun[101], K. Suruliz[156], C.J.E. Suster[157], M.R. Sutton[156], S. Suzuki[82], M. Svatos[141], M. Swiatlowski[37], S.P. Swift[2], T. Swirski[177], A. Sydorenko[100], I. Sykora[28a], M. Sykora[143], T. Sykora[143], D. Ta[100], K. Tackmann[46,z], J. Taenzer[161], A. Taffard[171], R. Tafirout[168a], R. Takashima[87], K. Takeda[83], T. Takeshita[150], E.P. Takeva[50], Y. Takubo[82], M. Talby[102], A.A. Talyshev[122b,122a], N.M. Tamir[161], J. Tanaka[163], M. Tanaka[165], R. Tanaka[65], S. Tapia Araya[173], S. Tapprogge[100], A. Tarek Abouelfadl Mohamed[136], S. Tarem[160], K. Tariq[60b], G. Tarna[27b,c], G.F. Tartarelli[69a], P. Tas[143], M. Tasevsky[141], T. Tashiro[86], E. Tassi[41b,41a], A. Tavares Delgado[140a], Y. Tayalati[35e], A.J. Taylor[50], G.N. Taylor[105], W. Taylor[168b], A.S. Tee[90], R. Teixeira De Lima[153], P. Teixeira-Dias[94], H. Ten Kate[36], J.J. Teoh[120], S. Terada[82], K. Terashi[163], J. Terron[99], S. Terzo[14], M. Testa[51], R.J. Teuscher[167,ad], S.J. Thais[183], T. Theveneaux-Pelzer[46], F. Thiele[40], D.W. Thomas[94], J.O. Thomas[42], J.P. Thomas[21], P.D. Thompson[21], L.A. Thomsen[183], E. Thomson[137], E.J. Thorpe[93], R.E. Ticse Torres[53], V.O. Tikhomirov[111,ak], Yu.A. Tikhonov[122b,122a], S. Timoshenko[112], P. Tipton[183], S. Tisserant[102], K. Todome[23b,23a], S. Todorova-Nova[143], S. Todt[48], J. Tojo[88], S. Tokár[28a], K. Tokushuku[82], E. Tolley[127], K.G. Tomiwa[33e], M. Tomoto[117], L. Tompkins[153,p], B. Tong[59], P. Tornambe[103], E. Torrence[132], H. Torres[48], E. Torró Pastor[148], C. Tosciri[135], J. Toth[102,ac], D.R. Tovey[149], A. Traeet[17], C.J. Treado[125], T. Trefzger[177], F. Tresoldi[156], A. Tricoli[29], I.M. Trigger[168a], S. Trincaz-Duvoid[136], D.A. Trischuk[175], W. Trischuk[167], B. Trocmé[58], A. Trofymov[145], C. Troncon[69a], F. Trovato[156], L. Truong[33c], M. Trzebinski[85], A. Trzupek[85], F. Tsai[46], J.C-L. Tseng[135], P.V. Tsiareshka[108,ag], A. Tsirigotis[162,w], V. Tsiskaridze[155], E.G. Tskhadadze[159a], M. Tsopoulou[162], I.I. Tsukerman[124], V. Tsulaia[18], S. Tsuno[82], D. Tsybychev[155], Y. Tu[63b], A. Tudorache[27b], V. Tudorache[27b], T.T. Tulbure[27a], A.N. Tuna[59], S. Turchikhin[80], D. Turgeman[180], I. Turk Cakir[4b,u], R.J. Turner[21], R.T. Turra[69a], P.M. Tuts[39], S. Tzamarias[162], E. Tzovara[100], G. Ucchielli[47], K. Uchida[163], F. Ukegawa[169], G. Unal[36], A. Undrus[29], G. Unel[171], F.C. Ungaro[105], Y. Unno[82], K. Uno[163], J. Urban[28b], P. Urquijo[105], G. Usai[8], Z. Uysal[12d], V. Vacek[142], B. Vachon[104], K.O.H. Vadla[134], A. Vaidya[95], C. Valderanis[114], E. Valdes Santurio[45a,45b], M. Valente[54], S. Valentinetti[23b,23a], A. Valero[174], L. Valéry[46], R.A. Vallance[21], A. Vallier[36], J.A. Valls Ferrer[174], T.R. Van Daalen[14], P. Van Gemmeren[6], I. Van Vulpen[120], M. Vanadia[74a,74b], W. Vandelli[36], M. Vandenbroucke[145], E.R. Vandewall[130], A. Vaniachine[166], D. Vannicola[73a,73b], R. Vari[73a], E.W. Varnes[7], C. Varni[55b,55a], T. Varol[158], D. Varouchas[65], K.E. Varvell[157], M.E. Vasile[27b], G.A. Vasquez[176], F. Vazeille[38], D. Vazquez Furelos[14], T. Vazquez Schroeder[36], J. Veatch[53], V. Vecchio[75a,75b], M.J. Veen[120], L.M. Veloce[167], F. Veloso[140a,140c], S. Veneziano[73a], A. Ventura[68a,68b], N. Venturi[36], A. Verbytskyi[115], V. Vercesi[71a], M. Verducci[72a,72b], C.M. Vergel Infante[79], C. Vergis[24], W. Verkerke[120], A.T. Vermeulen[120], J.C. Vermeulen[120], M.C. Vetterli[152,ap], N. Viaux Maira[147d], M. Vicente Barreto Pinto[54], T. Vickey[149], O.E. Vickey Boeriu[149], G.H.A. Viehhauser[135], L. Vigani[61b], M. Villa[23b,23a], M. Villaplana Perez[3], E. Vilucchi[51], M.G. Vincter[34], G.S. Virdee[21], A. Vishwakarma[46], C. Vittori[23b,23a], I. Vivarelli[156], M. Vogel[182], P. Vokac[142], S.E. von Buddenbrock[33e], E. Von Toerne[24], V. Vorobel[143], K. Vorobev[112], M. Vos[174], J.H. Vossebeld[91], M. Vozak[101], N. Vranjes[16], M. Vranjes Milosavljevic[16], V. Vrba[142], M. Vreeswijk[120], R. Vuillermet[36], I. Vukotic[37], P. Wagner[24], W. Wagner[182], J. Wagner-Kuhr[114], S. Wahdan[182], H. Wahlberg[89], V.M. Walbrecht[115], J. Walder[90], R. Walker[114], S.D. Walker[94], W. Walkowiak[151], V. Wallangen[45a,45b], A.M. Wang[59], A.Z. Wang[181], C. Wang[60c], F. Wang[181],

JHEP07(2020)124

H. Wang[18], H. Wang[3], J. Wang[63a], J. Wang[61b], P. Wang[42], Q. Wang[129], R.-J. Wang[100], R. Wang[60a], R. Wang[6], S.M. Wang[158], W.T. Wang[60a], W. Wang[15c], W.X. Wang[60a], Y. Wang[60a], Z. Wang[60c], C. Wanotayaroj[46], A. Warburton[104], C.P. Ward[32], D.R. Wardrope[95], N. Warrack[57], A. Washbrook[50], A.T. Watson[21], M.F. Watson[21], G. Watts[148], B.M. Waugh[95], A.F. Webb[11], S. Webb[100], C. Weber[183], M.S. Weber[20], S.A. Weber[34], S.M. Weber[61a], A.R. Weidberg[135], J. Weingarten[47], M. Weirich[100], C. Weiser[52], P.S. Wells[36], T. Wenaus[29], T. Wengler[36], S. Wenig[36], N. Wermes[24], M.D. Werner[79], M. Wessels[61a], T.D. Weston[20], K. Whalen[132], N.L. Whallon[148], A.M. Wharton[90], A.S. White[106], A. White[8], M.J. White[1], D. Whiteson[171], B.W. Whitmore[90], W. Wiedenmann[181], C. Wiel[48], M. Wielers[144], N. Wieseotte[100], C. Wiglesworth[40], L.A.M. Wiik-Fuchs[52], H.G. Wilkens[36], L.J. Wilkins[94], H.H. Williams[137], S. Williams[32], C. Willis[107], S. Willocq[103], I. Wingerter-Seez[5], E. Winkels[156], F. Winklmeier[132], O.J. Winston[156], B.T. Winter[52], M. Wittgen[153], M. Wobisch[96], A. Wolf[100], T.M.H. Wolf[120], R. Wolff[102], R. Wölker[135], J. Wollrath[52], M.W. Wolter[85], H. Wolters[140a,140c], V.W.S. Wong[175], N.L. Woods[146], S.D. Worm[21], B.K. Wosiek[85], K.W. Woźniak[85], K. Wraight[57], S.L. Wu[181], X. Wu[54], Y. Wu[60a], T.R. Wyatt[101], B.M. Wynne[50], S. Xella[40], Z. Xi[106], L. Xia[178], X. Xiao[106], I. Xiotidis[156], D. Xu[15a], H. Xu[60a], H. Xu[60a], L. Xu[29], T. Xu[145], W. Xu[106], Z. Xu[60b], Z. Xu[153], B. Yabsley[157], S. Yacoob[33a], K. Yajima[133], D.P. Yallup[95], N. Yamaguchi[88], Y. Yamaguchi[165], A. Yamamoto[82], M. Yamatani[163], T. Yamazaki[163], Y. Yamazaki[83], Z. Yan[25], H.J. Yang[60c,60d], H.T. Yang[18], S. Yang[60a], T. Yang[63c], X. Yang[60b,58], Y. Yang[163], W-M. Yao[18], Y.C. Yap[46], Y. Yasu[82], E. Yatsenko[60c,60d], H. Ye[15c], J. Ye[42], S. Ye[29], I. Yeletskikh[80], M.R. Yexley[90], E. Yigitbasi[25], K. Yorita[179], K. Yoshihara[137], C.J.S. Young[36], C. Young[153], J. Yu[79], R. Yuan[60b,h], X. Yue[61a], M. Zaazoua[35e], B. Zabinski[85], G. Zacharis[10], E. Zaffaroni[54], J. Zahreddine[136], A.M. Zaitsev[123,aj], T. Zakareishvili[159b], N. Zakharchuk[34], S. Zambito[59], D. Zanzi[36], D.R. Zaripovas[57], S.V. Zeißner[47], C. Zeitnitz[182], G. Zemaityte[135], J.C. Zeng[173], O. Zenin[123], T. Ženiš[28a], D. Zerwas[65], M. Zgubič[135], B. Zhang[15c], D.F. Zhang[15b], G. Zhang[15b], H. Zhang[15c], J. Zhang[6], L. Zhang[15c], L. Zhang[60a], M. Zhang[173], R. Zhang[181], S. Zhang[106], X. Zhang[60b], Y. Zhang[15a,15d], Z. Zhang[63a], Z. Zhang[65], P. Zhao[49], Z. Zhao[60a], A. Zhemchugov[80], Z. Zheng[106], D. Zhong[173], B. Zhou[106], C. Zhou[181], M.S. Zhou[15a,15d], M. Zhou[155], N. Zhou[60c], Y. Zhou[7], C.G. Zhu[60b], C. Zhu[15a,15d], H.L. Zhu[60a], H. Zhu[15a], J. Zhu[106], Y. Zhu[60a], X. Zhuang[15a], K. Zhukov[111], V. Zhulanov[122b,122a], D. Zieminska[66], N.I. Zimine[80], S. Zimmermann[52], Z. Zinonos[115], M. Ziolkowski[151], L. Živković[16], G. Zobernig[181], A. Zoccoli[23b,23a], K. Zoch[53], T.G. Zorbas[149], R. Zou[37], L. Zwalinski[36]

[1] *Department of Physics, University of Adelaide, Adelaide; Australia.*

[2] *Physics Department, SUNY Albany, Albany NY; United States of America.*

[3] *Department of Physics, University of Alberta, Edmonton AB; Canada.*

[4] [(a)] *Department of Physics, Ankara University, Ankara;* [(b)] *Istanbul Aydin University, Application and Research Center for Advanced Studies, Istanbul;* [(c)] *Division of Physics, TOBB University of Economics and Technology, Ankara; Turkey.*

[5] *LAPP, Université Grenoble Alpes, Université Savoie Mont Blanc, CNRS/IN2P3, Annecy; France.*

[6] *High Energy Physics Division, Argonne National Laboratory, Argonne IL; United States of America.*

[7] *Department of Physics, University of Arizona, Tucson AZ; United States of America.*

[8] *Department of Physics, University of Texas at Arlington, Arlington TX; United States of America.*

[9] *Physics Department, National and Kapodistrian University of Athens, Athens; Greece.*

[10] *Physics Department, National Technical University of Athens, Zografou; Greece.*

[11] *Department of Physics, University of Texas at Austin, Austin TX; United States of America.*

[12] [(a)] *Bahcesehir University, Faculty of Engineering and Natural Sciences, Istanbul;* [(b)] *Istanbul Bilgi University, Faculty of Engineering and Natural Sciences, Istanbul;* [(c)] *Department of Physics, Bogazici University, Istanbul;* [(d)] *Department of Physics Engineering, Gaziantep University, Gaziantep; Turkey.*

JHEP07(2020)124

[13] Institute of Physics, Azerbaijan Academy of Sciences, Baku; Azerbaijan.
[14] Institut de Física d'Altes Energies (IFAE), Barcelona Institute of Science and Technology, Barcelona; Spain.
[15] [(a)] Institute of High Energy Physics, Chinese Academy of Sciences, Beijing;[(b)] Physics Department, Tsinghua University, Beijing;[(c)] Department of Physics, Nanjing University, Nanjing;[(d)] University of Chinese Academy of Science (UCAS), Beijing; China.
[16] Institute of Physics, University of Belgrade, Belgrade; Serbia.
[17] Department for Physics and Technology, University of Bergen, Bergen; Norway.
[18] Physics Division, Lawrence Berkeley National Laboratory and University of California, Berkeley CA; United States of America.
[19] Institut für Physik, Humboldt Universität zu Berlin, Berlin; Germany.
[20] Albert Einstein Center for Fundamental Physics and Laboratory for High Energy Physics, University of Bern, Bern; Switzerland.
[21] School of Physics and Astronomy, University of Birmingham, Birmingham; United Kingdom.
[22] [(a)] Facultad de Ciencias y Centro de Investigaciónes, Universidad Antonio Nariño, Bogotá;[(b)] Departamento de Física, Universidad Nacional de Colombia, Bogotá, Colombia; Colombia.
[23] [(a)] INFN Bologna and Universita' di Bologna, Dipartimento di Fisica;[(b)] INFN Sezione di Bologna; Italy.
[24] Physikalisches Institut, Universität Bonn, Bonn; Germany.
[25] Department of Physics, Boston University, Boston MA; United States of America.
[26] Department of Physics, Brandeis University, Waltham MA; United States of America.
[27] [(a)] Transilvania University of Brasov, Brasov;[(b)] Horia Hulubei National Institute of Physics and Nuclear Engineering, Bucharest;[(c)] Department of Physics, Alexandru Ioan Cuza University of Iasi, Iasi;[(d)] National Institute for Research and Development of Isotopic and Molecular Technologies, Physics Department, Cluj-Napoca;[(e)] University Politehnica Bucharest, Bucharest;[(f)] West University in Timisoara, Timisoara; Romania.
[28] [(a)] Faculty of Mathematics, Physics and Informatics, Comenius University, Bratislava;[(b)] Department of Subnuclear Physics, Institute of Experimental Physics of the Slovak Academy of Sciences, Kosice; Slovak Republic.
[29] Physics Department, Brookhaven National Laboratory, Upton NY; United States of America.
[30] Departamento de Física, Universidad de Buenos Aires, Buenos Aires; Argentina.
[31] California State University, CA; United States of America.
[32] Cavendish Laboratory, University of Cambridge, Cambridge; United Kingdom.
[33] [(a)] Department of Physics, University of Cape Town, Cape Town;[(b)] iThemba Labs, Western Cape;[(c)] Department of Mechanical Engineering Science, University of Johannesburg, Johannesburg;[(d)] University of South Africa, Department of Physics, Pretoria;[(e)] School of Physics, University of the Witwatersrand, Johannesburg; South Africa.
[34] Department of Physics, Carleton University, Ottawa ON; Canada.
[35] [(a)] Faculté des Sciences Ain Chock, Réseau Universitaire de Physique des Hautes Energies - Université Hassan II, Casablanca;[(b)] Faculté des Sciences, Université Ibn-Tofail, Kénitra;[(c)] Faculté des Sciences Semlalia, Université Cadi Ayyad, LPHEA-Marrakech;[(d)] Faculté des Sciences, Université Mohamed Premier and LPTPM, Oujda;[(e)] Faculté des sciences, Université Mohammed V, Rabat; Morocco.
[36] CERN, Geneva; Switzerland.
[37] Enrico Fermi Institute, University of Chicago, Chicago IL; United States of America.
[38] LPC, Université Clermont Auvergne, CNRS/IN2P3, Clermont-Ferrand; France.
[39] Nevis Laboratory, Columbia University, Irvington NY; United States of America.
[40] Niels Bohr Institute, University of Copenhagen, Copenhagen; Denmark.
[41] [(a)] Dipartimento di Fisica, Università della Calabria, Rende;[(b)] INFN Gruppo Collegato di Cosenza, Laboratori Nazionali di Frascati; Italy.
[42] Physics Department, Southern Methodist University, Dallas TX; United States of America.

JHEP07(2020)124

[43] Physics Department, University of Texas at Dallas, Richardson TX; United States of America.
[44] National Centre for Scientific Research "Demokritos", Agia Paraskevi; Greece.
[45] [(a)] Department of Physics, Stockholm University; [(b)] Oskar Klein Centre, Stockholm; Sweden.
[46] Deutsches Elektronen-Synchrotron DESY, Hamburg and Zeuthen; Germany.
[47] Lehrstuhl für Experimentelle Physik IV, Technische Universität Dortmund, Dortmund; Germany.
[48] Institut für Kern- und Teilchenphysik, Technische Universität Dresden, Dresden; Germany.
[49] Department of Physics, Duke University, Durham NC; United States of America.
[50] SUPA - School of Physics and Astronomy, University of Edinburgh, Edinburgh; United Kingdom.
[51] INFN e Laboratori Nazionali di Frascati, Frascati; Italy.
[52] Physikalisches Institut, Albert-Ludwigs-Universität Freiburg, Freiburg; Germany.
[53] II. Physikalisches Institut, Georg-August-Universität Göttingen, Göttingen; Germany.
[54] Département de Physique Nucléaire et Corpusculaire, Université de Genève, Genève; Switzerland.
[55] [(a)] Dipartimento di Fisica, Università di Genova, Genova; [(b)] INFN Sezione di Genova; Italy.
[56] II. Physikalisches Institut, Justus-Liebig-Universität Giessen, Giessen; Germany.
[57] SUPA - School of Physics and Astronomy, University of Glasgow, Glasgow; United Kingdom.
[58] LPSC, Université Grenoble Alpes, CNRS/IN2P3, Grenoble INP, Grenoble; France.
[59] Laboratory for Particle Physics and Cosmology, Harvard University, Cambridge MA; United States of America.
[60] [(a)] Department of Modern Physics and State Key Laboratory of Particle Detection and Electronics, University of Science and Technology of China, Hefei; [(b)] Institute of Frontier and Interdisciplinary Science and Key Laboratory of Particle Physics and Particle Irradiation (MOE), Shandong University, Qingdao; [(c)] School of Physics and Astronomy, Shanghai Jiao Tong University, KLPPAC-MoE, SKLPPC, Shanghai; [(d)] Tsung-Dao Lee Institute, Shanghai; China.
[61] [(a)] Kirchhoff-Institut für Physik, Ruprecht-Karls-Universität Heidelberg, Heidelberg; [(b)] Physikalisches Institut, Ruprecht-Karls-Universität Heidelberg, Heidelberg; Germany.
[62] Faculty of Applied Information Science, Hiroshima Institute of Technology, Hiroshima; Japan.
[63] [(a)] Department of Physics, Chinese University of Hong Kong, Shatin, N.T., Hong Kong; [(b)] Department of Physics, University of Hong Kong, Hong Kong; [(c)] Department of Physics and Institute for Advanced Study, Hong Kong University of Science and Technology, Clear Water Bay, Kowloon, Hong Kong; China.
[64] Department of Physics, National Tsing Hua University, Hsinchu; Taiwan.
[65] IJCLab, Université Paris-Saclay, CNRS/IN2P3, 91405, Orsay; France.
[66] Department of Physics, Indiana University, Bloomington IN; United States of America.
[67] [(a)] INFN Gruppo Collegato di Udine, Sezione di Trieste, Udine; [(b)] ICTP, Trieste; [(c)] Dipartimento Politecnico di Ingegneria e Architettura, Università di Udine, Udine; Italy.
[68] [(a)] INFN Sezione di Lecce; [(b)] Dipartimento di Matematica e Fisica, Università del Salento, Lecce; Italy.
[69] [(a)] INFN Sezione di Milano; [(b)] Dipartimento di Fisica, Università di Milano, Milano; Italy.
[70] [(a)] INFN Sezione di Napoli; [(b)] Dipartimento di Fisica, Università di Napoli, Napoli; Italy.
[71] [(a)] INFN Sezione di Pavia; [(b)] Dipartimento di Fisica, Università di Pavia, Pavia; Italy.
[72] [(a)] INFN Sezione di Pisa; [(b)] Dipartimento di Fisica E. Fermi, Università di Pisa, Pisa; Italy.
[73] [(a)] INFN Sezione di Roma; [(b)] Dipartimento di Fisica, Sapienza Università di Roma, Roma; Italy.
[74] [(a)] INFN Sezione di Roma Tor Vergata; [(b)] Dipartimento di Fisica, Università di Roma Tor Vergata, Roma; Italy.
[75] [(a)] INFN Sezione di Roma Tre; [(b)] Dipartimento di Matematica e Fisica, Università Roma Tre, Roma; Italy.
[76] [(a)] INFN-TIFPA; [(b)] Università degli Studi di Trento, Trento; Italy.
[77] Institut für Astro- und Teilchenphysik, Leopold-Franzens-Universität, Innsbruck; Austria.
[78] University of Iowa, Iowa City IA; United States of America.
[79] Department of Physics and Astronomy, Iowa State University, Ames IA; United States of America.
[80] Joint Institute for Nuclear Research, Dubna; Russia.

JHEP07(2020)124

[81] [(a)] Departamento de Engenharia Elétrica, Universidade Federal de Juiz de Fora (UFJF), Juiz de Fora;[(b)] Universidade Federal do Rio De Janeiro COPPE/EE/IF, Rio de Janeiro;[(c)] Universidade Federal de São João del Rei (UFSJ), São João del Rei;[(d)] Instituto de Física, Universidade de São Paulo, São Paulo; Brazil.
[82] KEK, High Energy Accelerator Research Organization, Tsukuba; Japan.
[83] Graduate School of Science, Kobe University, Kobe; Japan.
[84] [(a)] AGH University of Science and Technology, Faculty of Physics and Applied Computer Science, Krakow;[(b)] Marian Smoluchowski Institute of Physics, Jagiellonian University, Krakow; Poland.
[85] Institute of Nuclear Physics Polish Academy of Sciences, Krakow; Poland.
[86] Faculty of Science, Kyoto University, Kyoto; Japan.
[87] Kyoto University of Education, Kyoto; Japan.
[88] Research Center for Advanced Particle Physics and Department of Physics, Kyushu University, Fukuoka ; Japan.
[89] Instituto de Física La Plata, Universidad Nacional de La Plata and CONICET, La Plata; Argentina.
[90] Physics Department, Lancaster University, Lancaster; United Kingdom.
[91] Oliver Lodge Laboratory, University of Liverpool, Liverpool; United Kingdom.
[92] Department of Experimental Particle Physics, Jožef Stefan Institute and Department of Physics, University of Ljubljana, Ljubljana; Slovenia.
[93] School of Physics and Astronomy, Queen Mary University of London, London; United Kingdom.
[94] Department of Physics, Royal Holloway University of London, Egham; United Kingdom.
[95] Department of Physics and Astronomy, University College London, London; United Kingdom.
[96] Louisiana Tech University, Ruston LA; United States of America.
[97] Fysiska institutionen, Lunds universitet, Lund; Sweden.
[98] Centre de Calcul de l'Institut National de Physique Nucléaire et de Physique des Particules (IN2P3), Villeurbanne; France.
[99] Departamento de Física Teorica C-15 and CIAFF, Universidad Autónoma de Madrid, Madrid; Spain.
[100] Institut für Physik, Universität Mainz, Mainz; Germany.
[101] School of Physics and Astronomy, University of Manchester, Manchester; United Kingdom.
[102] CPPM, Aix-Marseille Université, CNRS/IN2P3, Marseille; France.
[103] Department of Physics, University of Massachusetts, Amherst MA; United States of America.
[104] Department of Physics, McGill University, Montreal QC; Canada.
[105] School of Physics, University of Melbourne, Victoria; Australia.
[106] Department of Physics, University of Michigan, Ann Arbor MI; United States of America.
[107] Department of Physics and Astronomy, Michigan State University, East Lansing MI; United States of America.
[108] B.I. Stepanov Institute of Physics, National Academy of Sciences of Belarus, Minsk; Belarus.
[109] Research Institute for Nuclear Problems of Byelorussian State University, Minsk; Belarus.
[110] Group of Particle Physics, University of Montreal, Montreal QC; Canada.
[111] P.N. Lebedev Physical Institute of the Russian Academy of Sciences, Moscow; Russia.
[112] National Research Nuclear University MEPhI, Moscow; Russia.
[113] D.V. Skobeltsyn Institute of Nuclear Physics, M.V. Lomonosov Moscow State University, Moscow; Russia.
[114] Fakultät für Physik, Ludwig-Maximilians-Universität München, München; Germany.
[115] Max-Planck-Institut für Physik (Werner-Heisenberg-Institut), München; Germany.
[116] Nagasaki Institute of Applied Science, Nagasaki; Japan.
[117] Graduate School of Science and Kobayashi-Maskawa Institute, Nagoya University, Nagoya; Japan.
[118] Department of Physics and Astronomy, University of New Mexico, Albuquerque NM; United States of America.
[119] Institute for Mathematics, Astrophysics and Particle Physics, Radboud University Nijmegen/Nikhef, Nijmegen; Netherlands.

JHEP07(2020)124

[120] Nikhef National Institute for Subatomic Physics and University of Amsterdam, Amsterdam; Netherlands.
[121] Department of Physics, Northern Illinois University, DeKalb IL; United States of America.
[122] [(a)] Budker Institute of Nuclear Physics and NSU, SB RAS, Novosibirsk;[(b)] Novosibirsk State University Novosibirsk; Russia.
[123] Institute for High Energy Physics of the National Research Centre Kurchatov Institute, Protvino; Russia.
[124] Institute for Theoretical and Experimental Physics named by A.I. Alikhanov of National Research Centre "Kurchatov Institute", Moscow; Russia.
[125] Department of Physics, New York University, New York NY; United States of America.
[126] Ochanomizu University, Otsuka, Bunkyo-ku, Tokyo; Japan.
[127] Ohio State University, Columbus OH; United States of America.
[128] Faculty of Science, Okayama University, Okayama; Japan.
[129] Homer L. Dodge Department of Physics and Astronomy, University of Oklahoma, Norman OK; United States of America.
[130] Department of Physics, Oklahoma State University, Stillwater OK; United States of America.
[131] Palacký University, RCPTM, Joint Laboratory of Optics, Olomouc; Czech Republic.
[132] Institute for Fundamental Science, University of Oregon, Eugene, OR; United States of America.
[133] Graduate School of Science, Osaka University, Osaka; Japan.
[134] Department of Physics, University of Oslo, Oslo; Norway.
[135] Department of Physics, Oxford University, Oxford; United Kingdom.
[136] LPNHE, Sorbonne Université, Université de Paris, CNRS/IN2P3, Paris; France.
[137] Department of Physics, University of Pennsylvania, Philadelphia PA; United States of America.
[138] Konstantinov Nuclear Physics Institute of National Research Centre "Kurchatov Institute", PNPI, St. Petersburg; Russia.
[139] Department of Physics and Astronomy, University of Pittsburgh, Pittsburgh PA; United States of America.
[140] [(a)] Laboratório de Instrumentação e Física Experimental de Partículas - LIP, Lisboa;[(b)] Departamento de Física, Faculdade de Ciências, Universidade de Lisboa, Lisboa;[(c)] Departamento de Física, Universidade de Coimbra, Coimbra;[(d)] Centro de Física Nuclear da Universidade de Lisboa, Lisboa;[(e)] Departamento de Física, Universidade do Minho, Braga;[(f)] Departamento de Física Teórica y del Cosmos, Universidad de Granada, Granada (Spain);[(g)] Dep Física and CEFITEC of Faculdade de Ciências e Tecnologia, Universidade Nova de Lisboa, Caparica;[(h)] Instituto Superior Técnico, Universidade de Lisboa, Lisboa; Portugal.
[141] Institute of Physics of the Czech Academy of Sciences, Prague; Czech Republic.
[142] Czech Technical University in Prague, Prague; Czech Republic.
[143] Charles University, Faculty of Mathematics and Physics, Prague; Czech Republic.
[144] Particle Physics Department, Rutherford Appleton Laboratory, Didcot; United Kingdom.
[145] IRFU, CEA, Université Paris-Saclay, Gif-sur-Yvette; France.
[146] Santa Cruz Institute for Particle Physics, University of California Santa Cruz, Santa Cruz CA; United States of America.
[147] [(a)] Departamento de Física, Pontificia Universidad Católica de Chile, Santiago;[(b)] Universidad Andres Bello, Department of Physics, Santiago;[(c)] Instituto de Alta Investigación, Universidad de Tarapacá;[(d)] Departamento de Física, Universidad Técnica Federico Santa María, Valparaíso; Chile.
[148] Department of Physics, University of Washington, Seattle WA; United States of America.
[149] Department of Physics and Astronomy, University of Sheffield, Sheffield; United Kingdom.
[150] Department of Physics, Shinshu University, Nagano; Japan.
[151] Department Physik, Universität Siegen, Siegen; Germany.
[152] Department of Physics, Simon Fraser University, Burnaby BC; Canada.
[153] SLAC National Accelerator Laboratory, Stanford CA; United States of America.
[154] Physics Department, Royal Institute of Technology, Stockholm; Sweden.

JHEP07(2020)124

[155] Departments of Physics and Astronomy, Stony Brook University, Stony Brook NY; United States of America.
[156] Department of Physics and Astronomy, University of Sussex, Brighton; United Kingdom.
[157] School of Physics, University of Sydney, Sydney; Australia.
[158] Institute of Physics, Academia Sinica, Taipei; Taiwan.
[159] [(a)] E. Andronikashvili Institute of Physics, Iv. Javakhishvili Tbilisi State University, Tbilisi;[(b)] High Energy Physics Institute, Tbilisi State University, Tbilisi; Georgia.
[160] Department of Physics, Technion, Israel Institute of Technology, Haifa; Israel.
[161] Raymond and Beverly Sackler School of Physics and Astronomy, Tel Aviv University, Tel Aviv; Israel.
[162] Department of Physics, Aristotle University of Thessaloniki, Thessaloniki; Greece.
[163] International Center for Elementary Particle Physics and Department of Physics, University of Tokyo, Tokyo; Japan.
[164] Graduate School of Science and Technology, Tokyo Metropolitan University, Tokyo; Japan.
[165] Department of Physics, Tokyo Institute of Technology, Tokyo; Japan.
[166] Tomsk State University, Tomsk; Russia.
[167] Department of Physics, University of Toronto, Toronto ON; Canada.
[168] [(a)] TRIUMF, Vancouver BC;[(b)] Department of Physics and Astronomy, York University, Toronto ON; Canada.
[169] Division of Physics and Tomonaga Center for the History of the Universe, Faculty of Pure and Applied Sciences, University of Tsukuba, Tsukuba; Japan.
[170] Department of Physics and Astronomy, Tufts University, Medford MA; United States of America.
[171] Department of Physics and Astronomy, University of California Irvine, Irvine CA; United States of America.
[172] Department of Physics and Astronomy, University of Uppsala, Uppsala; Sweden.
[173] Department of Physics, University of Illinois, Urbana IL; United States of America.
[174] Instituto de Física Corpuscular (IFIC), Centro Mixto Universidad de Valencia - CSIC, Valencia; Spain.
[175] Department of Physics, University of British Columbia, Vancouver BC; Canada.
[176] Department of Physics and Astronomy, University of Victoria, Victoria BC; Canada.
[177] Fakultät für Physik und Astronomie, Julius-Maximilians-Universität Würzburg, Würzburg; Germany.
[178] Department of Physics, University of Warwick, Coventry; United Kingdom.
[179] Waseda University, Tokyo; Japan.
[180] Department of Particle Physics, Weizmann Institute of Science, Rehovot; Israel.
[181] Department of Physics, University of Wisconsin, Madison WI; United States of America.
[182] Fakultät für Mathematik und Naturwissenschaften, Fachgruppe Physik, Bergische Universität Wuppertal, Wuppertal; Germany.
[183] Department of Physics, Yale University, New Haven CT; United States of America.

[a] Also at Borough of Manhattan Community College, City University of New York, New York NY; United States of America.
[b] Also at CERN, Geneva; Switzerland.
[c] Also at CPPM, Aix-Marseille Université, CNRS/IN2P3, Marseille; France.
[d] Also at Département de Physique Nucléaire et Corpusculaire, Université de Genève, Genève; Switzerland.
[e] Also at Departament de Fisica de la Universitat Autonoma de Barcelona, Barcelona; Spain.
[f] Also at Department of Applied Physics and Astronomy, University of Sharjah, Sharjah; United Arab Emirates.
[g] Also at Department of Financial and Management Engineering, University of the Aegean, Chios; Greece.

JHEP07(2020)124

[h] Also at Department of Physics and Astronomy, Michigan State University, East Lansing MI; United States of America.
[i] Also at Department of Physics and Astronomy, University of Louisville, Louisville, KY; United States of America.
[j] Also at Department of Physics, Ben Gurion University of the Negev, Beer Sheva; Israel.
[k] Also at Department of Physics, California State University, East Bay; United States of America.
[l] Also at Department of Physics, California State University, Fresno; United States of America.
[m] Also at Department of Physics, California State University, Sacramento; United States of America.
[n] Also at Department of Physics, King's College London, London; United Kingdom.
[o] Also at Department of Physics, St. Petersburg State Polytechnical University, St. Petersburg; Russia.
[p] Also at Department of Physics, Stanford University, Stanford CA; United States of America.
[q] Also at Department of Physics, University of Adelaide, Adelaide; Australia.
[r] Also at Department of Physics, University of Fribourg, Fribourg; Switzerland.
[s] Also at Dipartimento di Matematica, Informatica e Fisica, Università di Udine, Udine; Italy.
[t] Also at Faculty of Physics, M.V. Lomonosov Moscow State University, Moscow; Russia.
[u] Also at Giresun University, Faculty of Engineering, Giresun; Turkey.
[v] Also at Graduate School of Science, Osaka University, Osaka; Japan.
[w] Also at Hellenic Open University, Patras; Greece.
[x] Also at IJCLab, Université Paris-Saclay, CNRS/IN2P3, 91405, Orsay; France.
[y] Also at Institucio Catalana de Recerca i Estudis Avancats, ICREA, Barcelona; Spain.
[z] Also at Institut für Experimentalphysik, Universität Hamburg, Hamburg; Germany.
[aa] Also at Institute for Mathematics, Astrophysics and Particle Physics, Radboud University Nijmegen/Nikhef, Nijmegen; Netherlands.
[ab] Also at Institute for Nuclear Research and Nuclear Energy (INRNE) of the Bulgarian Academy of Sciences, Sofia; Bulgaria.
[ac] Also at Institute for Particle and Nuclear Physics, Wigner Research Centre for Physics, Budapest; Hungary.
[ad] Also at Institute of Particle Physics (IPP), Vancouver; Canada.
[ae] Also at Institute of Physics, Azerbaijan Academy of Sciences, Baku; Azerbaijan.
[af] Also at Instituto de Fisica Teorica, IFT-UAM/CSIC, Madrid; Spain.
[ag] Also at Joint Institute for Nuclear Research, Dubna; Russia.
[ah] Also at Louisiana Tech University, Ruston LA; United States of America.
[ai] Also at Manhattan College, New York NY; United States of America.
[aj] Also at Moscow Institute of Physics and Technology State University, Dolgoprudny; Russia.
[ak] Also at National Research Nuclear University MEPhI, Moscow; Russia.
[al] Also at Physics Department, An-Najah National University, Nablus; Palestine.
[am] Also at Physics Dept, University of South Africa, Pretoria; South Africa.
[an] Also at Physikalisches Institut, Albert-Ludwigs-Universität Freiburg, Freiburg; Germany.
[ao] Also at The City College of New York, New York NY; United States of America.
[ap] Also at TRIUMF, Vancouver BC; Canada.
[aq] Also at Universita di Napoli Parthenope, Napoli; Italy.
[*] Deceased

JHEP07(2020)124